RADIOLOGICAL SURVEY AND ELEMENTAL ANALYSIS IN THE GOLD MINING BELT, SOUTHERN NYANZA, KENYA.

BY

ODUMO, BENJAMIN OKANG'
B.Sc. (Hons)

A THESIS SUBMITTED FOR EXAMINATION IN PARTIAL FULFILLMENTS OF THE REQUIREMENTS FOR THE AWARD OF DEGREE OF MASTER OF SCIENCE (PHYSICS) OF UNIVERSITY OF NAIROBI
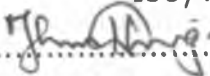
© 2009

i

DECLARATION

This thesis is my own work and has not been examined or submitted for examination in any other university.

Odumo, Benjamin Okang'

I56/7894/2005

Signature...................................Date...07/08/2009

This thesis has been submitted for examination with the approval of my supervisors.
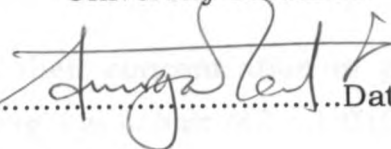
Prof. J.P. Patel

Department of Physics

University of Nairobi

Signature.................Date......06/08/09

and

Dr. A.O. Mustapha

Department of Physics

University of Nairobi

Signature.........................Date...05/8/09

Abstract

A radiological survey and elemental analysis in the gold mining belt was carried out at Osiri, Mikei, Masara and Macalder goldmines in Macalder Division of Migori district, in southern Nyanza, Kenya, where gold has been mined since 1920s. This was after it was realized that none of the previous studies in the region had considered radionuclide activity and elemental flux measured. This study aimed to provide data and information on the radiological as well as elemental impact of gold mining. To achieve this gold ore, water, sediments and dust from the mines were collected and analysed.

Elemental analysis of rock, water, sediment and dust samples was done using the ED-XRF technique. Activity concentration of ^{226}Ra in water samples was measured using liquid scintillation counting (LSC) spectrometry and the activity concentrations of ^{40}K and the decay products of ^{232}Th and ^{226}Ra were measured using gamma - ray spectrometry. Relevant exposure scenarios and pathways were identified and the doses received from these pathways were estimated by calculations based on generic dosimetric models. Measurement of dust loading at the various ore crushing sites was carried out by trapping the dust particles on a 0.45 micron cellulose acetate filter paper of 47 mm diameter using a vacuum pump. Absorbed doses in air at the mining sites, crushing sites and panning sites were evaluated from the measured activities of the radionuclides in these samples.

The major elements and their concentration in gold ore and sediments are: titanium (711 – 13,000) mg/kg; cobalt (83 - 1,010) mg/kg; zinc (30 – 63,210) mg/kg;; gold (14 - 73) mg/kg; copper (40-118,533) and mercury (16 - 150) mg/kg. Lead and arsenic were also available in high quantities. The major elements and their concentrations in the water samples on the other hand were: copper (29 - 14,976) µg /l; zinc (34 - 683) µg/l, lead and arsenic were

also detectable in higher quantities. Iron and magnesium were detected in all the dust levels.

The activity concentrations of ^{40}K, ^{226}Ra and ^{232}Th range from (80 - 413) Bq/Kg, (12- 145) Bq/Kg and (21 - 258) Bq/Kg with mean values of 100, 25 and 41 Bq/Kg, respectively. The ^{226}Ra in water samples was found to be below the detection limit (LD= 0.94 kBq m^{-3}).

The dust loading at Masara was found to be 3.668 mg/m^3 while the dust loading at Mikei was found to vary between (0.843 - 1.650) mg/m^3 with a mean of 1.334 mg/m^3.

The absorbed dose was found to range from 16 - 178 nGy/h with a mean of 42 nGy/h. The total calculated effective dose from the three exposure scenarios considered ranged from 0.7 - 4.2 µSv y^{-1}. The most significant pathway is the inhalation of the auriferous ore dust while the least significant is the external dose due to gamma-rays emitted by the radionuclides contained in the mining environment.

The activity concentration of the radionuclides as well as the annual absorbed dose were found to be below the worlds average while presence of toxic elements like arsenic, lead and zinc in high quantities were also noted. Inhalation of the gold ore dust was found to be the worst exposure pathway with crushing being the worst exposure scenario to the artisanal miners.

AKNOWLEDGEMENT

TABLE OF CONTENTS

Page

Chapter One

Introduction

Chapter Two

Literature Review

Chapter Three

Materials and Methods

Chapter Four

Results and Discussion

Chapter Five

Conclusions and Recommendations

Chapter Six

References

DEDICATION

I dedicate this work to my late father Odumo and late sisters Julia and Debora.

LIST OF TABLES

LIST OF FIGURES

LIST OF ABBREVIATIONS AND ACRONYMS

ASM: Artisanal Mining

BDL: Below Detection Limit

ED-XRF: Energy Dispersive X- ray Fluorescence

GDP: Gross Domestic Product

IAEA: International Atomic Energy Agency

LLD: Lower Limit of Detection

LSA: Liquid Scintillation Analysis

LSC: Liquid Scintillation Counter

NORM: Naturally Occurring Radioactive Materials

TENORM: Technologically Enhanced Naturally Occurring Radioactive
            Materials.

UNSCEAR: United Nations Scientific Committee on the Effects of Atomic
            Radiation

WHO: World Health Organization

Mac: Macalder (Makalda)

Osi: Osiri

Mik: Mikei

Mas: Masara

CHAPTER ONE

1.0 Introduction

1.1 Background of the study

All living organisms are exposed to ionizing radiation either from natural or man-made radioactive sources. The natural sources of radiation are of terrestrial and extra terrestrial origin. Terrestrial radiation is due to radioactive nuclides, ^{40}K, ^{232}Th and ^{238}U, present in varying amounts in soils, rocks and atmosphere while extra terrestrial radiation originates from the outer space as primary cosmic rays. The major manmade exposures are from nuclear reactors, X-ray and other radiation generators used for medical, industrial and other activities.

Background exposures from normal levels of the naturally occurring radioactive materials (NORM) are present in all environmental materials (soils, rocks, water, food) and do not vary remarkably from place to place. The average effective dose is about 2.4 mSv/y (UNSCEAR, 2000). Where human activities, due to burning of coal, mining and others have increased the relative concentration of the radionuclides in such materials, they are referred to as the technologically enhanced naturally occurring radioactive materials (TENORM). Higher exposures arise from such human activities because they involve extraction and disposal of large quantities of materials containing ^{40}K and other radionuclides in the decay series of ^{232}Th and ^{238}U.

Miners may be occupationally exposed to radiations during extraction, transportation and processing of the minerals. They may experience internal exposures to radon, thoron (and their short-lived decay products) and other radionuclides in the airborne or ingestible dust and external exposures to gamma and beta radiations from their surroundings. Exposure of the general public living near the mines may also arise from radionuclides which may be directly ingested through drinking water or uptake through the food chain with

1

vegetables, fish, milk, meat etc. Exposure of the public may also result from the reuse of the mine wastes (tailings and mine waters).

Apart from the radiological problems, mining is also associated with other non-radiological problems such as pollution and land degradation. A number of studies conducted in gold mining areas of the Witwatersrand showed increasing evidence that mines frequently contaminate adjacent environments with heavy metals, salts and radionucides. In cases where nearby streams are affected, high rates of downstream transportation and the contamination of soil and sediments far away from the source of pollution are possible (Winde and Sadham, 2004). Heavy metals are of particular interest for a number of reasons. Firstly, they show a tendency to accumulate in the sediments and the soils and have a long persistence time, since they are non biodegradable. Secondly, they are ubiquitous in sediments and soil arising from both natural and anthropogenic sources with pathways including inheritance from the parent rocks, application of water as well as local and long range atmospheric and fluvial deposits of emissions from dust and mining (Getaneh and Alemayehu, 2006).

Trace amounts of metals can be found in minerals constituting mineralized rocks. The size reduction process like crushing, during ore processing increases the surface area of the reaction of rock/mineral particles thereby accelerating oxidation and/or chemical weathering and hence the release of metals. Many of the metals are essential at low concentrations to plants, animals and human health but at higher concentrations they can be toxic. In some cases the concentration of metals in different environmental media can exceed the maximum tolerable concentration and can cause harm to life. A number of case histories have been documented and reported from different parts of the world (Ogola et al., 2002).

This study therefore focused mainly on occupational exposure to radiation from NORMS during mining of gold by artisans in Macalder, Mikei, Osiri and Masara

in Macalder division in Migori district, but also considered the non radiological aspects of the mining risks. To quantify both radiological and non-radiological risks, measurement of the dust loading, activity of radionuclides and elemental concentration in the ores, sediments, dust and waters from the mines were carried out using nuclear and atomic analytical techniques.

1.2 *Geology and mineralization of Migori gold mining belt*

According to Shackleton (1946), the rocks in Migori are Archaean in age, about 2.8 million years old (Figure 1). They are referred to as the Migori granite green stone. The Archaean rocks of Migori district are known to contain gold. Gold occurs in quartz veins within the mafic volcanics of the nyanzian group. The host rocks are metabasalt, banded ironstone, shales and andesites. Two hypotheses are advanced for gold sulphide mineralization in the region. Shackleton (1946) considered the presence of apophytes and veined ore bodies within the host rocks at Macalder to be indicative of a hydrothermal-metasomatic origin. However, Sanders (1964), suggested that gold mineralization in the deposit took place in a pre-existing thrust structure. In contrast, Hutchson (1981) concluded that Macalder is a deformed volcanogenic massive sulphide deposit of a primitive type, which was formed over a sea floor hydrothermal vent. Factors favouring synegenetic hypothesis include sheet like ore bodies within the host rocks. In the Macalder deposit, Ogola (1987) noted that the emplacement of gold within the host rocks was due to epigenetic vein type mineralization and the mode of formation is volcanogenic hydrothermal. Keays (1982) reckons that most vein type Archaean gold deposits probably formed after the deformation and metamorphism of the host rocks, apparently, due to late stage metamorphic fluids.

The mineralization fluids apparently, were generated during the granite intrusion. The latter might have played the role of a heat engine during which there was dissolution of the elements followed by subsequent concentration and redeposition of minerals within tectonically favorable environments.

3

Figure 1. The Geological map Of Migori Goldbelt (Sanders, 1964)

Several studies have been carried out on the gold mining in Kenya. For example the impact of gold mining on the environment and human health in the Migori gold mining belt was studied by Ogola et al. (2002), another study had also been carried out on gender and mining in Kenya: the case of Mukibira mines in Vihiga district (Amutabi et al., 2001) etc. However, none of the previous studies has considered the radiological impact of the gold mining processes. The miners and the relevant government authorities are therefore unaware of the possible radiological risks that the miners are exposed to during the gold mining activities. This present study is therefore designed to investigate the possible radiological impact of gold mining by artisans in Macalder division, Migori district.

1.3 Objectives of the study

1.3.1 General objective

The overall goal of this study was to investigate, using spectrometric techniques, the radiological exposure and elemental flux aspects of artisanal gold mining activities in the Osiri, Mikei, Masara and Macalder in gold mining areas in Migori District's gold mining belt.

1.3.2 Specific objectives

The specific objectives were to:

i. Measure the activity concentration of radionuclides in ores and sediments obtained from the mines and the panning sites at Macalder, Mikei, Osiri and Masara in Macalder division in Migori district.

ii. Measure the level of ^{226}Ra in mine water.

iii. Measure the elemental concentration in the sediments, ores, dust, and water from the mines.

iv. Measure dust loading in the mining sites.

v. Calculate the absorbed dose of radiation in air in the mines.

vi.   Calculate effective dose from various exposure pathways.

1.4 *Justification and significance of the study*

This study will provide useful information and data on the radiological aspect of mining which hitherto were not available since all previous studies were focused on the non radiological impacts. The study is therefore expected to create awareness to all the stake holders including (artisanal) miners, the local population, as well as the relevant regulatory authorities on the impact of mining operation. This will therefore provide basis for further action.

CHAPTER TWO

2.0 LITERATURE REVIEW

2.1 *Naturally occurring radioactive materials (NORM) in mining*

All minerals and raw materials contain radionuclides of natural, terrestrial origin- these are commonly referred to as primordial radionuclides. The ^{238}U and ^{232}Th decay series and ^{40}K are the main radionuclides of interest. The activity concentrations of these radionuclides in normal rocks and soils are variable but generally low. However certain minerals, including some that are commercially exploited contain uranium and/or thorium radionuclides at significantly elevated activity concentrations. By industrial, physical, chemical and thermal processes, the natural equilibrium of the radionuclides can be disturbed resulting in either an enrichment or decrease of some radionuclides compared to the original matrix.

A study in the Majingu phosphate mine in Tanzania found high concentration of ^{226}Ra in phosphate rock, 5760 ± 107 Bq/kg and waste rock 4250 ± 98 Bq/kg while surface waters had an activity concentration of 4.7 ± 0.4 Bq/l (Banzi *et al., 1999*). Banzi *et al.* (1999) also found the absorbed dose rate in air to be of the average of 1415 nGy/h which led to estimation of annual dose to be about 12mSv/y. This is about 12 times higher than the recommended dose for the members of the public by ICRP. A similar study carried out in two gold mines in Sudan however found lower annual effective dose ranging from 0.01 to 0.2 mSv/y while the absorbed dose ranged from 2.2 to 32.3 nGy/h (Sam and Awad, 2000). Sam and Awad (2000) further found the concentration of ^{226}Ra and ^{232}Th to be increasing in the order soil>spoil heap> ore.

Miners in underground mines are more exposed to radiations compared to their counterparts on the surface mines as was found in Brazil and Ghana respectively (Veiga and Hinton, 2002; Darko *et al.*, 2005). A study of the gold mines by Darko *et al.* (2005) in Ghana while determining occupational

exposure to NORMS from surface and underground mines in the Ashanti region in Ghana found the miners in the underground mines are exposed to an annual effective dose of 1.83 ± 0.56 mSv/y compared to surface miners who were exposed to a dose of only 0.26 ± 0.11 mSv/y. The high radiation exposure in the underground mines is mainly due to Radon gas which is transported to the galleries through water and air circulation during mining. Results of a study of the coal mines in Brazil also indicated that the inhalation of radon progeny may be a source of occupational exposure (Lipsztein *et al.*, 2001): the study found significant levels of uranium in a coal miner's urine. The study however, found the concentrations of uranium, thorium and ^{210}Po in the mines to be below detection limits. The study also identified ingestion to be the most important pathway for thorium intake; this finding however contradicts the study by Abbady *et al.*(2005) and Mustapha *et al.*(2007) that found inhalation of dust to be the most significant pathway (Abbady *et al.*, 2005; Mustapha *et al.*, 2007).

Measurements of ambient radiation and determination of radionuclide concentrations in mining wastes and soils in former uranium and radium mines showed that mud from the neutralization ponds used to treat acid mine waters contain elevated radioactive concentrations. The study further found that in mill tailings in the mining facilities where the radioactive ore was chemically extracted, contain elevated levels of radioactivity, up to 200 times normal levels (Carvalho *et al.*, 2007). This raises a lot of concern especially in the areas like Migori gold belt where the miners and general public more often use tailings from the gold mines to construct their houses.

Gold miners are exposed to radiation from different exposure scenarios like during extraction, sieving, panning and crushing of the ore etc. On the other hand the exposure pathways include external irradiation by gamma rays emitted by radionuclides contained in the ground; external exposure from submission in air contaminated by auriferous dust; internal irradiation due to

inhalation of auriferous dust in the air; and internal irradiation due to inadvertent ingestion of auriferous dust (Mustapha *et al.*, 2007).

Chemical and physical processes during gold mining and extraction, particularly when carried out in conjunction with uranium extraction and sulphuric acid manufacture, act on the uranium minerals and the radioactive decay products of uranium. The sequence of the processing steps may have a significant influence on the movement of the radioactive materials (Wendel, 1998). Water as used in gold mining process also plays an important role in moving naturally occurring radionuclides through the environment, both as a transport medium for the bulk ore and as a medium for chemical reactions.

2.2 *Elemental concentration in mining materials*

Drainage waters from gold mine tailings and adits from Kilimafesa mine in Tanzania, former gold and copper mine, showed the presence of heavy metals like aluminum, arsenic, copper, iron, lead, manganese and zinc in higher concentrations with their levels ranging from 21 mg/l to 622 mg/l (Bowell *et al*, 1995). They also found the concentration of the metals to be more in the waters from tailings than the adits. Presence of the same metals was also registered in gold mines in Kenya and Ethiopia by Ogola *et al.* (2002) and Getaneh and Alemayehu (2006), respectively. Ogola *et al.* (2005) in addition found the level of mercury to be high in their study: this high level of mercury can be explained from the fact that mercury is used in gold amalgamation by the artisanal miners in the Migori gold mining belt as is also used in Australia, Brazil and several other places all over the world (Veiga and Hinton, 2002). These studies however did not register the presence of uranium at elevated levels as was registered in the gold mining areas of the Witwatersrand (Winde and Sandtham, 2004) and those located in eastern Johannesburg (Rösner and Schackwyk, 2000) in the Republic of South Africa.

2.3 *Artisanal gold mining in Kenya*

Artisanal gold mining started several years ago, for example in India it is dated back to 400BC (Deb *et al.,* 2008). Early artisanal mining early was also reported in Brazil, Portugal etc, where the artisanal miners are referred to as the *garimpeiros* (Veiga and Hinton, 2002). In Africa, gold mining has also been carried out for years, for instance in the Witwatersrand and Johannesburg in South Africa and in the Ashanti region in Ghana and other places.

Mining in Kenya accounts for less than 1 % of the country's gross domestic product (GDP). Kenya has been known in the east African region for the production of non metallic minerals such as diatomite, fluorspar, limestone, salt, soda ash, and vermiculite, as well as a variety of gemstones and materials for construction. A feasibility study completed recently estimated reserves of mineralized sands at Kwale to be 140 million metric tons (Mt) (Bemeüdez, 1999).

Gold mining in Kenya has been going on for close to a century and is now being carried out primarily by the artisanal miners. There are several gold deposits present in Kenya; of late there has been a renewed attempt by different companies to explore gold in Southwestern Kenya. The major regions in focus have been Lolgorian in Transmara district and Macalder division in Migori district. The gold in this region is believed to be embedded in the Lake Victoria greenstone belt, which is also responsible for gold mining ventures in adjoining Tanzania (Shackleton, 1946).

Artisanal mining (ASM) refers to mining by individuals, groups, families or groups with minimal or no mechanization in the informal (sometimes illegal) sector of the market (Hetschel *et al.,* 2002). According to the recent International Labor Organization (ILO) survey, about 13 million people are involved in Artisanal mining producing 15 to 20 % of the world's non-fuel mineral resources (ILO, 1999). Small scale gold mining activity is not unique

to Kenya only; it is widely spread throughout Africa, Latin America and Asia (Hilson, 2002). Artisanal mining is popular with gold because it has an advantage of being relatively simple to extract, refine and transport. Small scale gold mining can only take place where mineralization occurs near the surface and within unconsolidated rocks, the most frequent being deposits contained in riverbed alluvium and colluviums, and altered upper portions of quartz veins. Recent increase in gold mining in Kenya has had positive impact on unemployment, but at the same time has a plethora of environmental implications.

Mercury pollution and land degradation are by far the two most serious environmental problems encountered in small scale gold mining today. Metallic mercury has for a long time been the preferred option for concentrating and extracting gold from low grade ores mainly because it is cheap, reliable and portable. It is now a well known fact that mercury, in sufficient quantities, poses a serious threat to human health and is deleterious to a wide range of ecological entities. Once in the natural environment, mercury undergoes a change of speciation from an inorganic form to a stable methylated state (MeHg) and when ingested, ecotoxicological impact results. Since it is readily transferred across the placenta, acute exposure causes animals to initially become anorexic and lethargic, after which muscles ataxia, motor control deficits and visual impairment develop with convulsions preceding death.

Small scale gold mining activity also causes significant damage to the landscapes. More specifically, as a migratory industry, small scale gold mining have been responsible for the removal of the vast quantities of surface vegetation and mass deforestation. Furthermore, miners typically abandon pits and trenches without properly reclaiming the spoils. It is therefore quite common to find, following periods of intensive prospecting, landscapes littered with potholes and virtually devoid of vegetation cover.

11

CHAPTER THREE

3.0 Materials and Methods

3.1 Sampling sites

Samples of ore, sediment, water and dust were collected from Osiri, Masara, Macalder (Makalda) and Mikei mining sites in southern Nyanza Kenya. The sampling locations are shown in Figure 2.

Figure 2. Location of the sampling sites.

3.2 Sample collection procedures

Ore, sediment, water and dust samples were collected from various mining sites at Mikei, Osiri, Macalder and Masara using various sample collection methods as described below.

3.2.1 Collection of ore samples

Thirteen samples including powder ore/crushed rocks were collected from panning sites, crushing sheds. Pieces of rocks identified to be ores ere also collected in the mines. In all cases about half kilogram of the sample was put in a well labeled plastic bag.

3.2.2 Collection of sediment samples

Thirteen sediment samples were collected from the panning sites both from the artificial ponds dug in the ground next to the crushing sheds and near river banks. They were also labeled appropriately. All the sediment samples were wet apart from the two dry samples from a heap that were left to dry near the ponds for reprocessing.

3.2.3 Collection of water samples

Eleven water samples were collected in 0.5 liter plastic bottles from various panning ponds and mines in Masara, Osiri, Mikei and Macalder. At each sampling point, the bottles were rinsed at least three times with the water before taking the sample. Each bottle was immersed to about 10 cm below the water surface to prevent aeration incase of presence of radon gas. The samples were tightly sealed and labeled: labeling included the time and date of sampling.

3.2.4 Collection of samples of air borne dust

Environmental air over the crushing sites was pumped through 0.45 µm air filters of diameter 47 mm. The pumping was carried out for about 30 minutes for each filter. The filters were weighed before and after exposures to evaluate the dust loading in the air during the sampling. Each of the ten filters collected were kept in a petri dish labeled with the weight before exposure and the sampling duration awaiting analysis after exposure.

3.3 Sample preparation

3.3.1 Preparation of ore and sediments for ED-XRF counting

In the laboratory, the ores and the sediments were dried in the open and then prepared as described below according to the requirements of the intended analytical technique:

i.   Each of the samples was first crushed and pulverized into fine powder.
ii.   The pulverized sample was then sieved to grain sizes of equal to or less than 100 (≤ 100) µm. Nylon sieve was used so as to avoid contamination of the sample.
iii. About 1 g of the fine sample was mixed with about 0.3 grams of cellulose to achieve a mass ratio of 1 (cellulose): 3 (sample) and divided into three portions and each portion pressed into a pellet of diameter 2.5 cm. The weight of the pellets obtained varied between 2.5 and 4.8 mg.

The pellets were labeled appropriately and kept in a petri dish to avoid contamination.

3.3.2 Preparation of water samples for ED-XRF analysis

100 ml of each water sample was preconcentrated to a pH of 3.5 by adding Nitric acid (HNO_3). Where the pH went below 3.5, ammonium solution was added to adjust it upwards to 3.5. 2 ml of 1 % ammonium-1-pyrolidonedithiocabomate (APDC) solution was then added to the preconcentrate before stirring for about 30 minutes. The filtrate of the preconcentrate was then collected over a 0.45 µm millipore filter paper of 47mm diameter and left to dry.

3.3.3 Preparation of samples for a gamma-ray spectroscopy

The remaining pulverized samples (ore and sediments) were sealed in 250 milliliter plastic containers for about one month. This was to allow gaseous radon (half life 3.8 days) and its short lived decay daughters (^{214}Bi and ^{214}Pb) to reach equilibrium with the long lived ^{226}Ra precursor in the sample. The sample weights ranged from 240.1 g to 564.8 g. A background sample was also prepared by filling a similar container with distilled water.

3.3.4 Preparation of samples for liquid scintillation counting

10 milliliters of each water sample was pippetted into a 22 ml vial. 10 ml of Opti Flour liquid scintillator (cocktail) was then added before mixing thoroughly by shaking and left to settle for about three hours. It was noticed that the mixture separated into two immiscible layers: the Opti Flour cocktail on top of the water. The samples were later analyzed with the liquid scintillation counter (LSC).

3.4 Analytical techniques

3.4.1 *Gamma-ray spectroscopy*

Gamma rays are high energy electromagnetic radiations emitted in the process of de-excitation of the atomic nucleus. Gamma rays from spontaneous nucleus decay are emitted with a rate and energy (colour) spectrum that is unique to the nuclear species that is decaying. The uniqueness provides the basis for most gamma ray assay techniques; by counting the number of gamma rays emitted with a specific energy it is possible to determine the types and number of the nuclei that emitted that radiation.

3.4.1.1 *Interaction of gamma-rays with matter*

Gamma rays must interact with the sample to be detected. Gamma-rays measured outside a sample is always attenuated because of gamma ray interaction with the sample.

3.4.1.2 *Fundamental law of attenuation*

When a gamma radiation of intensity I_0 is incident on an absorber of thickness L, the emerging radiation of intensity I transmitted by the absorber is given by the exponential expression

$$I = I_o e^{-\mu_t L}$$

(1)

μ_t is the attenuation coefficient

The attenuation coefficient depends on the gamma-ray energy and the atomic number, Z, and the density, ρ, of the absorber.

Gamma-rays react primarily with the atomic electrons; therefore, the attenuation coefficient must be proportional to electron density ρ, which is proportional to bulk density of the absorbing material. However, for a given

16

material the ratio of the element density to the bulk density is constant, Z/A, independent of bulk density. The ration Z/A is nearly constant for all except the heavy elements.

The ratio of linear attenuation coefficient to the density μ_ℓ/ρ is called the mass attenuation coefficient μ.

$$\mu = \frac{N_o \sigma}{A} \qquad (2)$$

N_o is Avogadro's number

A is the atomic weight

σ is the interaction cross section.

Mass attenuation is independent of density and is commonly used since it quantifies the gamma-ray interaction probability of an individual element.

3.4.1.2.1 Interaction processes

The gamma rays interact with detectors and absorbers by three by major processes, photoelectric absorption Compton scattering and pair production (Figure 3).
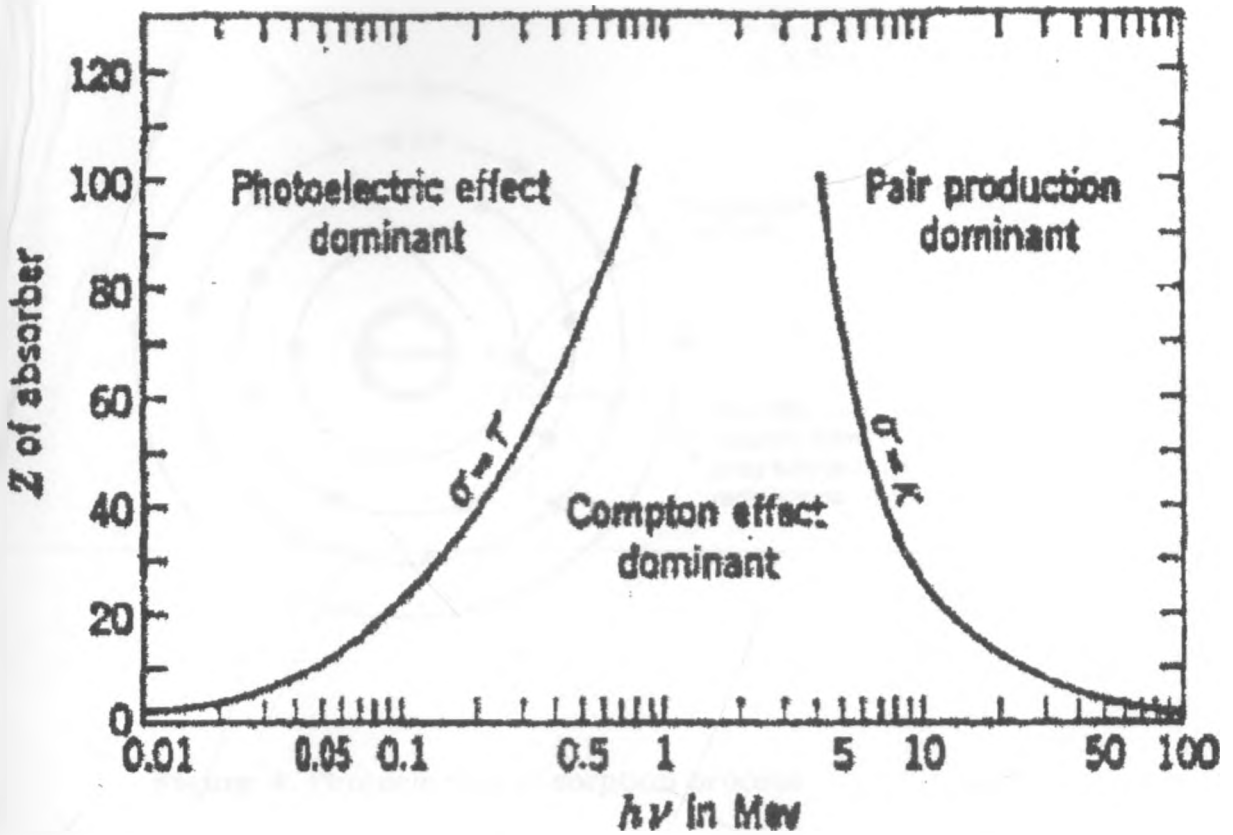
Figure 3. The three major types of gamma-ray interaction with matter (Knoll, 1979).

a) *Photoelectric absorption*

A gamma- ray may interact with a bound electron in such a way that it looses all its energy to the target electron and the electron is ejected from the atom (Figure 4).

18
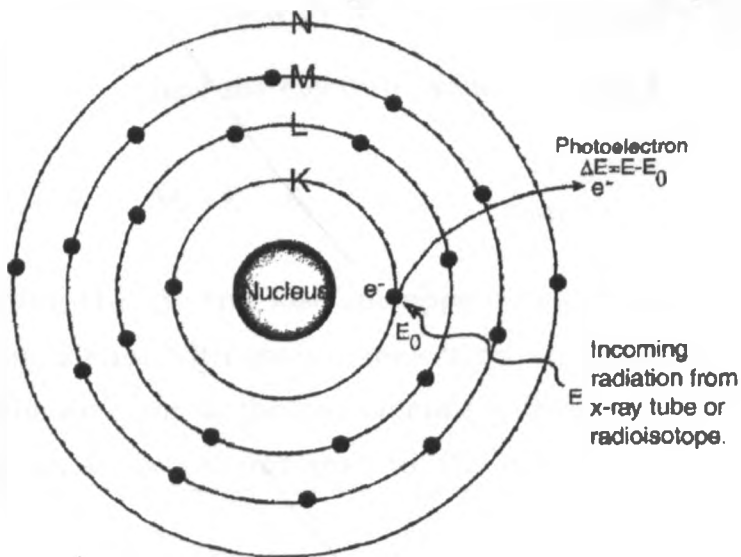
Figure 4. Photoelectric absorption process

ne of the energy is used to overcome the electron binding energy and most
he remainder to free the electron as kinetic energy. A very small amount of
oil energy remains with the atom to conserve the momentum.

otoelectric absorption for gamma-ray detection, because the gamma-ray
s all its energy, the resulting pulse falls within the full energy peak. The
bability of photoelectric absorption depends on the gamma–ray energy, the
ctron binding energy and the atomic number of the atom. The probability of
otoelectric absorption is probability greater for most tightly bound electrons.
erefore the K electrons are the most affected. The probability of photoelectric
iorption is given equation

$$\tau\alpha\frac{Z^4}{E^3}$$

(3)

e energy of the electron released by the interaction is the difference between

e gamma-ray energy E and the electron binding energy E_o.

$$\Delta E = E - E_o \qquad\qquad (4)$$

ıe electron binding energy isn't lost but appears as the characteristic X-rays
ɪitted in the coincidence with the photoelectron. In most cases, these X-rays
ɪe absorbed in the detector in the coincidence with the photoelectron and the
sulting output pulse is proportional to the total energy of the incident
ɪmma-ray.

Compton scattering

ɔmpton scattering is the process whereby gamma-ray interacts with a free or
weakly bound electron (Figure 5). The incident gamma-ray with energy,
$\rangle\rangle E$, transfers part of its binding energy to the electron.
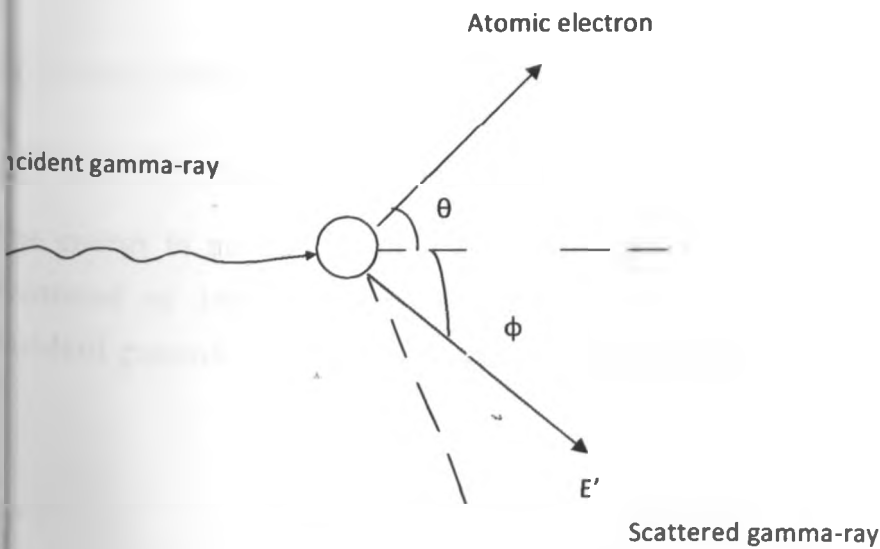
Figure 5. Schematic diagram of Compton scattering process.

The interaction involves the outer least tightly bound electron in the scattering atom. The electron becomes a free electron with kinetic energy equal to the difference of the energy lost by the gamma-rays and the electron bonding energy. Because the electron binding energy is very small compared to the gamma-ray energy, the kinetic energy of the electron is nearly equal to the energy lost by the incident gamma-ray.

$$E_e = E - E' \tag{5}$$

E_e is the energy of scattered electron

E is the energy of the incident gamma-ray

E' is the energy of scattered gamma ray

The direction of the electron and the scattered gamma-ray depend on the amount of energy transferred to the electron during interaction.

$$E' = \frac{M_o c^2}{(1 - \cos\theta + M_o c^2 / E)} \tag{6}$$

$M_o c^2$ is the rest energy of the electron, 511 keV.

θ angle between the incident and scattered gamma-ray.

The energy is minimum for a head on scattered collision where gamma-ray is scattered at 180^0 and the electron moves forward in the direction of the incident gamma-ray. In this case the scattered gamma-ray is given by

$$E'_{(min)} = \frac{M_o c^2}{(2 + M_o c^2 / E)} \tag{7}$$

21

for very small scattering angles ($\Phi \cong 0^{\circ}$) the energy of the scattered gamma-rays is only slightly less than the energy of the incident gamma-ray and the scattered electron takes very small energy away from the interaction. When Compton scattering in a detector, the detection medium and the detector produces an output pulse that is proportional to the energy lost by the incident gamma-ray because Compton scattering involves the least tightly bound electrons, the nucleus has a minor influence and the probability of interaction is nearly independent of atomic number. The interaction probability depends on electron density, which is proportional to Z/A and nearly constant for all materials. The Compton Scattering probability is a slowly varying function of gamma-ray energy.

c) Pair production

A gamma-ray with energy of at least 1.022 meV can create an electron-positron pair when the influence of strong electromagnetic field is in the vicinity the nucleus (Figure 6).
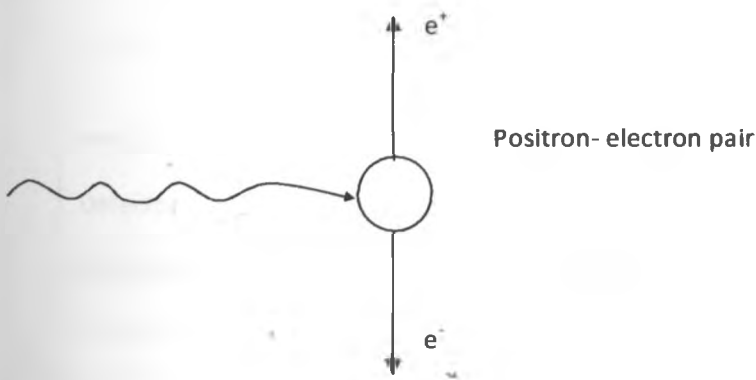
Figure 6. Schematic diagram of pair production process.

n this interaction the nucleus receives a very small amount of recoil energy to conserve the momentum, but the nucleus is otherwise unchanged and the gamma-rays disappear. This interaction has a thresh hold of 1.022 MeV because that is the minimum energy required to create the electron-positron pair. If the gamma-ray exceeds 1.022 MeV, the excess energy is shared between the positron and the electron as kinetic energy. This interaction process is relatively unimportant of nuclear assay because most of the important gamma-ray signatures are below 1.022 MeV. The electron -positron product are slowed down in the absorber.

After losing its kinetic energy, the positron combines with the electron in annihilation process, which releases gamma-ray with energies of 0.511 MeV. These lower energy gamma-rays may interact further with absorbing material or may escape.

Pair production is possible for gamma-rays with energy less 1.022 MeV. Above this threshold, the probability of the interaction increases rapidly with energy. The probability of pair production varies approximately as the square of the atomic number Z and is significant in high Z elements.
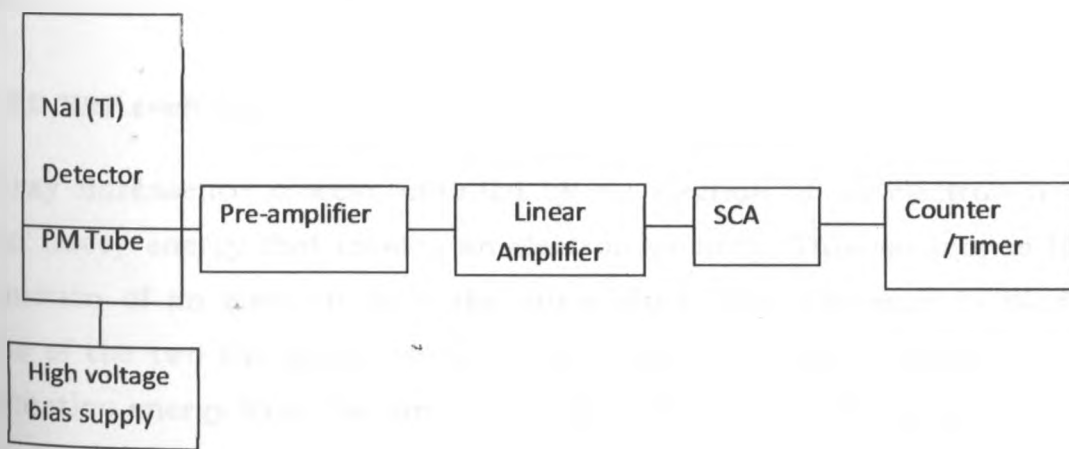
Figure 7. Block diagram of a Single-Channel-Analyzer (SCA) with NaI (TI) detector.

The samples were analyzed using a gamma-ray spectrometer consisting of a HP 5583A single channel analyzer (SCA) model, consisting of NaI(Tl) detector attached to photomultiplier tube (PM), Hewlett Packard (HP) 5580B NM power supply, HP 5582A linear amplifier, HP 5590A scale and a timer (Figure 7). Each sample was placed directly on the NaI(Tl) detector of the Single Channel Analyzer (SCA) and counted in each of the three windows calibrated at between channel numbers 4.0 and 4.5 for ^{40}K (1460 keV), 5.0 and 5.5 for ^{214}Bi (1764 keV) and 8.0 to 8.5 for ^{208}Tl (2615 keV) for 8 hours. Calibration was done using reference materials provided by the International Atomic Energy Agency (IAEA) namely RGU-1, RGTh-1 and RGK-1 (Oyedele, 2006). The true counts for each window were obtained after subtracting the background counts in each window obtained by running background sample (distilled water) in the same geometry for 8 hours. To calculate the activity concentration of each sample, a secondary standard called RgMix2 was also run for the same duration and the counts noted for each window. From the true counts obtained from the RgMix2 and from its known activity concentration, i.e. 5721 Bq/kg for ^{40}K, 1012 Bq/kg for ^{226}Ra and 1269 Bq/kg for ^{232}Th, the method of proportion was used to estimate the activity concentration of the ore and sediment samples.

3.4.2 ED-XRF technique

The X-ray flurescence process initiated by an ejection of an electron by an external force/ energy that creates an electron vacancy. This vacancy is filled by transition of an electron from the outer shell. The difference in binding energies of the two electrons results in the creation of characteristic X-rays. The excitation energy from the inner atom may also be transferred to the outer electrons causing it to be ejected from the atom, such an electron is called Auger electron. Because each atom has a unique pattern, with its electrons having distinct quantum number, the resulting characteristic X-rays are also unique with specific frequency and acts as fingerprints of elements in XRF

analysis. The emission of characteristic radiation can be induced by the impact of accelerated particles such as electrons, protons, alpha particles and ions; or by the impact of high energy radiation from an X-ray tube or suitable radioactive source. In this work, Cadmium (^{109}Cd) was used.

3.4.2.1 Quantitative analysis in ED-XRF, general expression

Generally, direct electron excitation is used in the electron microprobe technique, while radioisotope sources and accelerator are commonly associated with energy dispersive technique. For reasons of sensitivity, the combination of the high power sealed X-ray tube and wavelength dispersion by selected crystal remains the practical and preferred technique for quantitative X-ray fluorescence (XRF) analysis.

In X-ray fluorescence analysis, it is the intensities of the radiation from a sample which is the basis of quantitative analysis. The energy spectrum consists of the characteristic X-ray lines and the background contributions due to coherent and incoherent scattering. The latter tend to interfere with quantitative analysis.

The geometry of the excitation source in relation to the sample and the detector is shown in Figure 8.
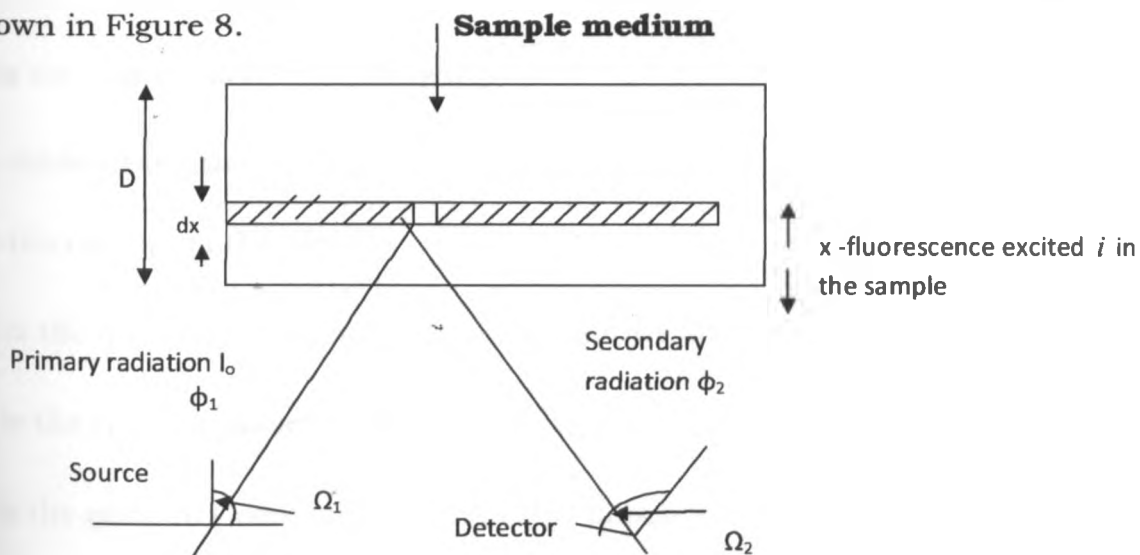
Figure 8. Interaction of X-rays with a sample

ϕ_1 is the incident angle of primary radiation with the sample

ϕ_2 is the emergent angle of secondary radiation with the sample

Ω_1 is the solid angle of the incident primary radiation as seen by the sample

Ω_2 is the solid angle of the emergent secondary radiation as seen by the detector.

The intensities are expressed in photons or X-ray counts per second. The dependence of the intensity of flourescent radiation of element i and its mass per unit area is according to Sparks (1979) given by:

$$I_i(E_i) = G_o.K_i.\varepsilon(E_i).\rho_i d_i \left[\frac{1 - \exp(a\rho d)}{a\rho d} \right] \qquad (8)$$

where

$I_i(E_i)$ is the measured fluorescence intensity of element i

$I_o = (E_i)$ is the intensity of primary exciting radiation

K_i is the relative detection efficiency

d is thickness of the sample

ρ is the density of the sample

$\rho_i d_i$ is the mass per unit area of element i in the sample

$\varepsilon(E_i)$ is the relative efficiency of the detector for photons of energy E_i.

G_o is the geometry constant which is also dependent on the source activity as is the case with radioisotope sources. G_o is given by the following equation

$$G_o = \frac{I_o(E_o)\Omega_1\Omega_2}{\sin\phi_1} \qquad (9)$$

and

$$K_i = \sigma_i^{ph}(E_o)\left(1 - \frac{1}{J_{is}}\right)\omega_{is}\cdot f_s^i\, E_o \qquad (10)$$

Where $\sigma_i^{ph}(E_o)$ is the photoelectric mass absorption coefficient of the element i at energy E_o .

ω_{is} is the fluorescent yield for element i in the "S".

$1 - \frac{1}{J_{is}}$ is the relative probability for photoelectric effect in shell "S".

f_s^i is the ratio of the intensity of a given K or L line to the intensity of the whole line series. The total mass absorption coefficient for primary and fluorescent X-ray radiation in the sample is given by

$$a = \mu(E_o)\csc\Omega_1 + \mu(E_1)\csc\Omega_2 \qquad (11)$$

where $\mu(E_o)$ and $\mu(E_1)$ are the total mass absorption coefficients in the sample at primary and secondary energies.

In the above equation it is assumed that:

- The sample is homogenous

- The excitation source is a point source

- The primary radiation is monochromatic

- The density of the element i, ρ, in the sample is constant over the whole volume

• Affixed geometry is maintained during the experiment i.e. Ω_1 and Ω_2 is constant.
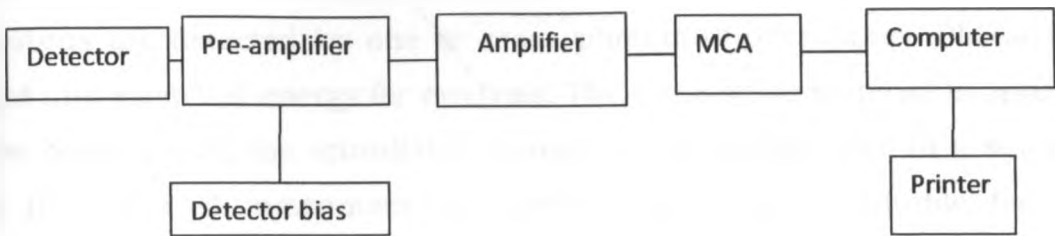
Figure 9. Block diagram of EX-DRF spectrometry

The ED-XRF spectrometer, Figure9, used in this study consisted of a X- ray generator as the excitation source operated at 35 volts and 20 mA; Canberra Si (Li) detector, an ORTEC spectroscopy shaping amplifier model 571, ORTEC high voltage supply bias model 475, ORTEC liquid nitrogen monitor and a Canberra multichannel analyzer (S-100), which measures the heights of different pulses and stores the results in memory counters called channels. The MCA is interfaced with a personal computer (Figure 4). The detector is maintained at liquid nitrogen temperature of 77K (~ -203ºC).

Each dust and water filter was run for 500 seconds while each pellet was run for 2000 seconds live time and the spectra collected by the Canberra detector with energy resolution of 195 eV for (Mn-K$_\alpha$) X-rays at 5.9 KeV. The characteristic X-ray spectra obtained from the samples were evaluated by non-linear least squares fitting using the analysis of X-ray spectra by the interactive least squares – quantitative X –ray analysis for thin samples (AXIL- QXAS) code.

3.4.3 Liquid Scintillation Counting (LSC)

In liquid scintillation analyzers, energy from emitted radiation is absorbed by a fluorescent material (scintillation flour) and is re- emitted as light photons. The light photons are detected by one or more photomultiplier tubes (PMTs) and converted into electrical energy for analysis. The radioactive material is brought into close contact with the scintillator, usually by dissolving both in a suitable solvent; this type of instrument is therefore particularly suitable for the qualitative measurement of radiation which has limited penetrating power, such as alpha particles, beta particles and soft X-rays. It also has a very short resolving time therefore high rates of disintegration can be measured.

The measurement of radioactivity by means of liquid scintillation counter involves two main stages. First, energy from the radiation excites molecules of a suitable solvent (primary solvent) and re-emitted as light (scintillation). Secondly, the emitted photons are detected by a photomultiplier tube and converted to electrical pulses (Figure 10).
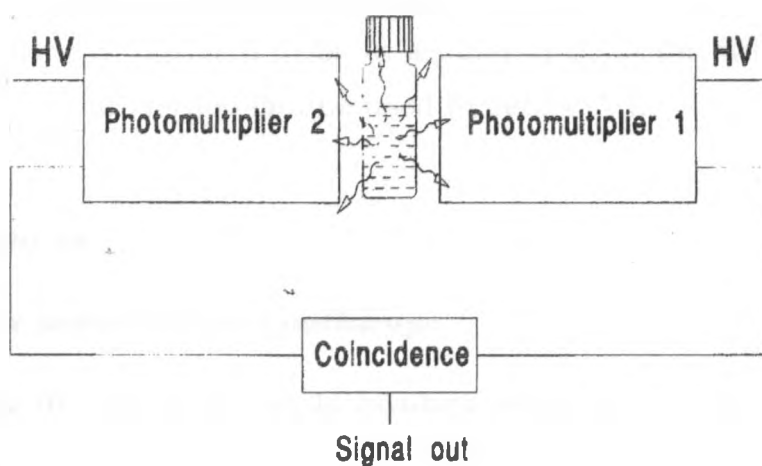
Figure 10. Block diagram of a scintillation counter.

The radioactive material whose activity is to be measured is mixed with a liquid scintillation cocktail in a transparent vial which is then lowered into the counting chamber situated between the two photomultiplier tubes of the liquid scintillation counter. The inside of the scintilator is surrounded by a lead shielding to exclude as much extraneous radiation as possible. Light delivered from scintillation in the counting vial enters the photomultiplier tubes either directly or after reflection from the walls of the chamber, whose internal surface is ligned with a reflecting material.

In this study, measurements were performed using the Packard Tri-Carb 1000 TR LSA interfaced with PC containing the Packard Applications Management system (AMS) and Spectragraph™ software packages. Each sample was counted for 5 minutes with a wide window setting of (25-900) in one of the three regions of the LSA. The background counting was done with de-ionized water for 600 minutes. The cocktail used in this study was Opti Flour. The advantage of Opti Flour as a cocktail is that radon (^{222}Rn) is 48 times more soluble in it than in water and the quenching effect it offers is uniform in all samples analysed, including background and standards, since most of the energy transfer takes place in the floating Opti Flour. Once ^{222}Rn is sealed for about one month it is expected to be in secular equilibrium with its precursor i.e. ^{226}Ra therefore the method can be used to detect ^{226}Ra.

3.5 Dose estimates

3.5.1 Exposure scenarios and pathways

Gold mining by the artisans mainly involves extraction of ore manually from open pits. The extracted ore is then left in the open to dry before crushing into fine grains using mallets. The fine grain is then sieved to get fine powder which is mixed with mercury at the panning sites. The panning can either be carried

out in a flowing river or in ponds dug close to the crushing sites. Mercury mixes with gold to form an amalgam which settles at the bottom of the trough used for panning while the rest of the sediments are gradually emptied into the pond/river. Excess mercury is separated from gold in the amalgam by hand-squeezing the piece of fabric on which the gold and mercury have settled. This recovered mercury is usually bottled for reuse. Further refinement of the gold obtained to remove any remaining mercury and water, is by burning directly in open air. The same process of gold extraction is reported in other countries e.g. India and Brazil as described by Deb *et al.* (2008) and Veiga and Hinton (2002), respectively. Based on the operations described above, the following exposure scenarios and pathways were considered for the dose assessment:

a) Exposure scenarios

   i.   Extracting and transporting the ore.

   ii. Crushing the ore.

   iii. Sieving the ore.

   iv. Panning the ore.

   v.   Drying the ore in open air.

   vi. Storing the ore.

b) Exposure pathways

   i.   External irradiation by γ- rays emitted from radionuclides contained in the ground, in the stock piles of ores or in the dust created during crushing and deposited on surfaces.

   ii. External exposure due to submersion in air contaminated with dust.

   iii. Internal irradiation due to inhalation of dust in the air.

   iv. Internal irradiation due to inadvertent ingestion of dust.

31

3.5.2 *Dose calculation procedures*

The radiation doses that are likely to accrue from each working or exposure scenario were calculated using existing generic models that closely describe exposure scenarios. Typical input parameters include the activity concentrations of the relevant radionuclides in various types of materials, working habit data (e.g. exposure duration, breathing rates, etc) and the dose coefficients. Information on the working and living habits were obtained by observing and interviewing the miners. Other parameters, including dose coefficients, were adopted from the open literature (Ekerman and Ryman, 1993; ICRP, 1994). For the calculations involving dust loading, the value of dust loading at Mikei was used.

The radiation doses that are likely to accrue from each exposure scenario were calculated as follows:

a). **External dose due to γ- rays emitted by radionuclides contained in the environment**

Calculation of the absorbed dose rate at 1 meter above the ground containing ^{40}K, ^{232}Th and ^{226}Ra, which were assumed to be uniformly distributed in the ground, is obtained using the relationship :

$$D = 0.666 A_{Th} + 0.042 A_K + 0.429 A_{Ra}$$

(12)

where D represents total absorbed dose in air nGyh^{-1}. A_{Th}, A_K and A_{Ra} are the activity concentrations of ^{232}Th, ^{40}K and ^{226}Ra respectively, present in the ore and sediment samples. The contents on the right hand side of the equation above are related to the average gamma-ray energies for each radionuclide or series. Dose conversion factor or dose coefficient represent the dose rate in air per unit activity concentration of radionuclides in the soil sample and is expressed in nGyh^{-1} per Bq/kg (Tahir *et al.*, 2005). The relationship was based on the dose conversion factors recommended by the UNSCEAR (1993), for the

32

estimation of the total air absorbed outdoor gamma radiation. It is noted that the calculation of these DCFs has been based on the assumption that the decay products of the ^{226}Ra and ^{232}Th series are in the radioactive equilibrium with their precursors (Sam and Elmahadi, 2007).

The external effective dose D_{ext} (Sv y^{-1}) received by an individual due to distribution of radionuclides in sediment, rock, ore or dust in the immediate environment was then calculated using the equation

$$D_{ext} = \sum_R A_R DC_{ext,R} T \qquad (13)$$

where A_R (Bqg^{-1}) is the activity concentration of gamma ray emitting radionuclides in the dust, sediment,... and $DC_{ext, R}$ is the effective dose coefficient of the radionuclide in Svh^{-1} per Bqg^{-1}. T is the exposure time in hours.

The external effective dose coefficients for external exposure to radionuclides including contributions from short lived daughters are shown in Table 1.

Table 1. Effective dose coefficients for external exposure to radionuclides including contributions from short-lived daughters (Mustapha *et al.*, 2007).

| Radionuclides | Effective dose coefficients (nSvh⁻¹ per Bqg⁻¹) | | | Contaminated Surface | Air Submersion (nSv h⁻¹ per Bqm⁻³) |
| | Soil contaminated to | | | | |
	1 cm	5 cm	Infinite Depth		
^{40}K	5.472	15.552	30.701	1.175	0.029
^{226}Ra	60.224	172.975	327.514	9.929	0.302
^{228}Ra	33.178	95.040	174.528	5.409	0.162
^{228}Th	51.553	148.951	298.616	8.299	0.276
^{230}Th	0.012	0.027	0.033	0.004	0
^{232}Th	0.006	0.012	0.014	0.003	0
^{234}U	0.005	0.009	0.011	0.003	0
^{238}U	1.205	2.467	3.700	0.668	0.005

b) **Internal dose due to inhalation of air contaminated with dust**

The weight of the accumulated dust was obtained by subtracting the pre-exposure weight of the filter from the post-exposure weight (Omar *et al.*, 2007). Dust loading therefore was calculated by

$$C_d = \frac{Z-Y}{V} \tag{14}$$

where C_d is the total dust loading (gm⁻³), Z and Y are the post and pre exposure filter weights (g) respectively while V is the volume of the air sampled (m³).

The effective dose due to inhalation of contaminated air with dust D_{inh} (Sv y⁻¹) was then calculated using the equation:

$$D_{inh} = \sum_R A_R DC_{inh,R} C_d I_w T \qquad (15)$$

where $DC_{inh,R}$ is the effective dose coefficient for radionuclide R $(nSvBq^{-1})$, I_w is the inhalation rate (1.2 m^3/h), and A_R is the activity concentration of radionuclides in the dust sample and T is as defined as above (eqn. 2). In order to apportion the mean alpha activity due to the ^{226}Ra and ^{232}Th chain nuclides, the average ratio of their activities present in the mineral was assumed to be present in the air borne inhaled dust (Haridasan *et al.*, 2006; Oatway and Mobbs, 2003).

Effective doses coefficients for inhalation and ingestion for selected radiocuclides including contributions from their short lived product is shown in Table 2.

Table 2. Effective doses per unit intake of selected radionuclides including contributions from their short-lived products (adopted from ICRP,1994). (Moderate (M) and Slow (S) absorption rates were selected for insoluble ores.)

Radionuclides	Committed effective dose per unit intake (nSv Bq^{-1})	
	By inhalation (absorption type)	By ingestion (fractional absorption)
^{226}Ra	5600 (M)	1200 (0.2)
^{228}Ra	1700 (M)	670 (0.2)
^{228}Th	34500 (S)	106 (0.0002)
^{230}Th	7200 (S)	87 (0.0002)
^{232}Th	12000 (S)	92 (0.0002)
^{234}U	6800 (S)	8 (0.002)
^{238}U	5700 (S)	12 (0.002)

c) Internal dose due to inadvertent ingestion of radionuclides

The effective dose D_{ing} (Sv y^{-1}) due to inadvertent ingestion of radionuclides was calculated using the equation

$$D_{ing} = \sum_R A_R DC_{ing,R} I_{w,ing} T$$

(16)

where $DC_{ing,R}$ is the effective dose coefficient for ingestion (SvBq^{-1}), $I_{w,ing}$ is the ingestion rate and all other terms have same meaning as described earlier. Inadvertent ingestion is assumed to occur through hand to mouth transfer of contaminated soil and dust present on the skin and clothing. For the purposes of this research the amount of soil that is likely to be inadvertently ingested by an adult in these working conditions is assumed to be 5×10^{-3} g/h (Oatway and Mobbs, 2003).

T was taken to be 780 hours in a year for a miner working for three hours for five days in a week for 52 weeks for the digging and panning scenarios. While for T for crushing was taken to be 1560 hours in a year i.e. a miner working for 6 hours for five days in a week for 52 weeks.

d) The total effective dose for each exposure scenario

The total annual effective dose, E_T, received by the artisans who dig and/or handle ores and slurries containing gold is the sum of the doses from external irradiation by gamma-rays emitted by radionuclides contained in the ground and the environment, inhalation of air contaminated by dust and inadvertent ingestion of radionuclides in dust. This is given by the equation

$$E_T = D_{ext} + D_{inh} + D_{ing}$$

(17)

36

CHAPTER FOUR

4.0 RESULTS AND DISCUSSION

Results of the analyses of the ore, sediment, water and dust samples are presented and discussed in the following sections

4.1 Detection limits

4.1.1: Calculation of the limit of detection of NaI(Tl)the single channel analyzer

The detection efficiency of radionuclide i was calculated using the formula

$$\varepsilon_i = \frac{n_S - n_B}{C.m_S.} \tag{18}$$

where ε_i (counts per second per Bq) is the absolute counting efficiency of gamma rays in the window of interest, n_S (counts per second) is the count rate recorded in the energy window when the sample holder is filled with the reference material (RgMix 2), n_B is the count rate in the same energy window when the sample holder is filled with distilled water, i.e. the background count, m_S is the mass of the RgMix 2 and C is the activity concentration of the radionuclide in RgMix 2 in Bq/Kg.

The limit of detection L_D (Bq/Kg) was therefore calculated using the equation (Mustapha, 1999).

$$L_D = \frac{1}{m_S.\varepsilon_i} \left(\frac{2.71}{T} + 4.65 \sqrt{\frac{C_B}{T}} \right) \tag{19}$$

37

where C_B is the count rate in the energy window of distilled water, the background, T (seconds) is the counting time and m_S (Kg) is the mass of the distilled water sample. For the mass of water, which was used as the background, the counting was done for 8 hours and the limit of detection of 40K, 226Ra and 232Th was found to be 43 Bq/Kg, 10 Bq/Kg and 14 Bq/Kg respectively.

The corresponding limit of detection of the absorbed dose was found to be 15 nGy/h with the calculation based on respective limits of detection of each radionuclide.

4.1.2 Calculation of the limit of detection of the liquid scintillation counter

The limit of detection of the liquid scintillation counter was calculated using the formula given by Mustapha (1999):-

$$L_D = \frac{1}{0.964\,K.\varepsilon.V} \left(\frac{2.71}{T} + 4.65\sqrt{\frac{C_B}{T}} \right) \qquad (20)$$

L_D is the lower limit of detection, K is a unit normalization constant equal to 60 seconds per minute, ε is counting efficiency, 0.964 is the fraction of 222Rn in the Opti Flour O cocktail in a vial of total capacity 22 ml, assuming it contains 10ml of Opti flour O, 10 ml water and 2 ml air, V is the volume of water (10 ml), T is the counting time (60 minutes in this study), C_B is the counts per minute (20 counts). The limit of detection in this case was found to be 0.94 kBq m^{-3}.

4.1.3 Calculation of the elemental limits of detection of the ED-XRF technique

The lower detection limits (LDL) for the various elements were calculated using the equation 10 (Phillips, 1981).

$$Det.Lim. = \frac{3.C\sqrt{N_B}}{N_P} \qquad (21)$$

where,

C is the concentration of the element (mg/kg).

N_P is the net peak area for the element

N_B is the net background area under the element peak.

The lower detection limit of detection is shown in Table 3.

4.2 Elemental concentration

4.2.1 Ores and sediments

The levels of some elements including titanium, zinc, iron, arsenic, lead, copper, cobalt and manganese were detectable in all the samples from all the mines investigated, a typical spectrum ED-XRF is shown in Figure 7. These elements have also been reported in the findings of Ogola et al. (2002). Ogola et al. (2002) analyzed sediments from the rivers, Migori and Macalder, passing through the mining areas. The level of iron in the present study is consistently high particularly in the Macalder mines, 105815 ± 24230-374216 ± 6853 mg/kg, where the values are in percentages compared to the rest of the mines. The highest level recorded at Macalder being 30 % as shown in Table 4. The level of copper in Macalder mine is equally higher than the other mines, and this underscores the reason copper was the main mineral of interest in the Macalder mines.

Table 3. Lower limits of detection of ore and sediment (mg/kg), dust samples (mg/m^3) and water (μg/l).

element	Lower Detection limit of ores and sediments (mg/kg)	Lower Detection limit of dust on filter (mg/m^3)	Lower limit of detection of water (μg/l)
K	350	-	-
Ca	270	-	-
Ti	165	-	30
Cr	106	3	25
Mn	86	2	15
Fe	70	2	10
Co	58	-	10
Cu	40	2	6
Zn	35	-	5
As	20	-	20
Br	15	-	-
Rb	11	-	-
Sr	5	-	-
Y	4	-	-
Zr	4	-	-
Nb	3	-	-
Au	10	-	-
Hg	2	-	-
Pb	4	-	10

Table 4. Elemental concentration of ores and sediment at Macalder (mg/kg).

Element	Mac- S 1	Mac- S 2	Mac- O 1	Mac- O 2	Mac- O 3	Mac- O 4	Mac- O 5
K	<350	<350	<350	<350	<350	<350	1326 ± 233
Ca	24733 ± 1900	30333 ± 2246	5706 ± 3910	22400 ± 1783	23153 ± 2096	3331 ± 572	1069 ± 130
Ti	3530 ± 409	4123 ± 439	3690 ± 408	3600 ± 426	<165	<165	2474 ± 175
Cr	1607 ± 151	1617 ± 154	1453 ± 1140	1917 ± 173	1220 ± 121	904 ± 99	368 ± 32
Mn	1363 ± 107	1277 ± 102	1113 ± 91	1657 ± 128	1638 ± 135	1106 ± 93	1433 ± 97
Fe	305000 ± 19767	265000 ± 17200	221333 ± 14333	366667 ± 23767	374216 ± 24230	256291 ± 16611	105815 ± 6853
Co	2533 ± 227	2093 ± 194	1653 ± 167	3733 ± 293	5734 ± 457	4332± 437	2891 ± 259
Cu	7443 ± 487	5620 ± 369	2973 ± 198	9103± 596	118533 ± 7711	1661 ± 128	6451 ± 424
Zn	8980 ± 586	6073 ± 397	1310 ± 89	11167 ± 728	11850 ± 775	63210 ± 4103	3805 ± 252
As	2763 ± 184	4310 ± 283	2513 ± 167	3623 ± 239	8427 ± 555	<20	1434± 98
Au	<10	<10	<10	<10	<10	<10	73 ± 2
Hg	<2	<2	<2	<2	<2	150 ± 35	<2
Pb	3137 ± 205	3503 ± 228	2687 ± 176	2967 ± 239	14999 ± 978	14670 ± 957	1552 ± 103
Br	<15	<15	<15	<15	62 ± 13	<15	<15
Sr	8 ± 2	12 ± 2	138 ± 10	<5	21 ± 4	<5	88 ± 7
Y	15 ± 2	20 ± 2	14 ± 2	16 ± 2	45 ± 6	83 ± 11	19 ± 3
Zr	23 ± 2	27 ± 2	27 ± 2	26 ± 2	19 ±4	<4	95± 7
Nb	<3	<3	<3	<3	<3	<3	29 ± 3

Key:

O- Ore;S- Sediment.

41
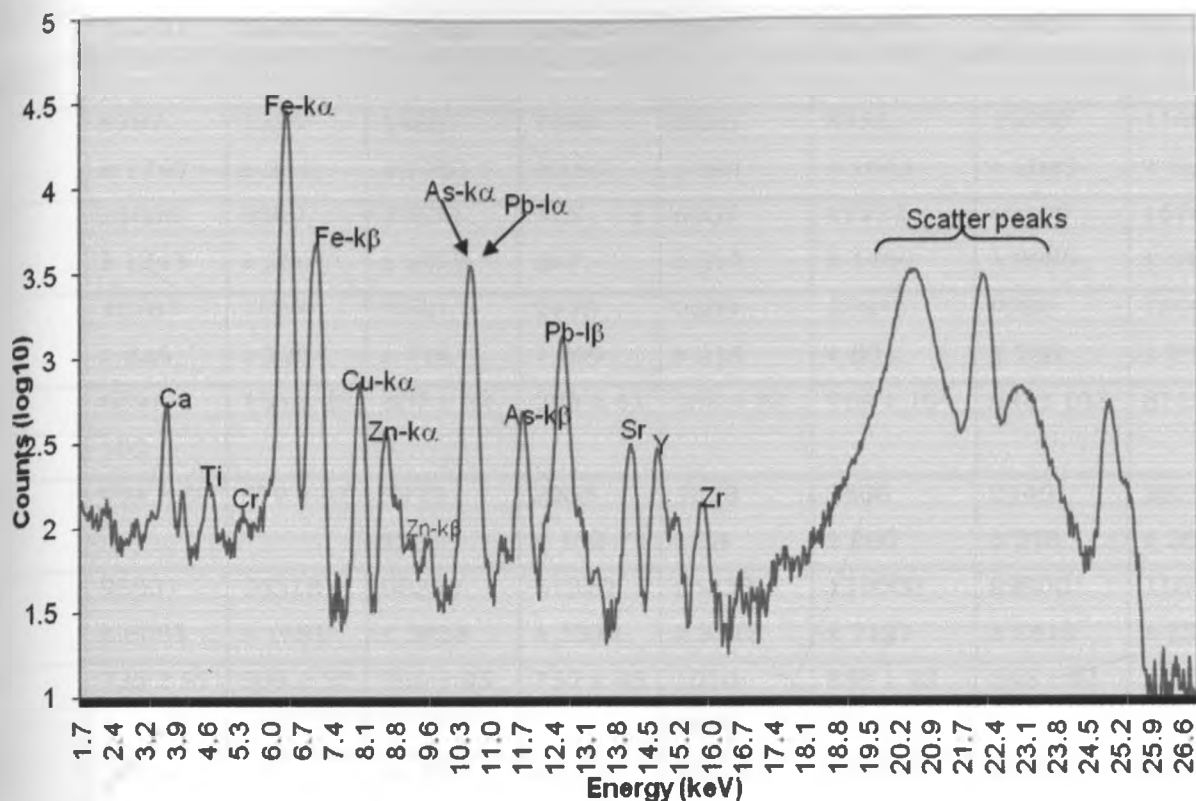
Figure 11. Typical ED-XRF spectrum of an ore sample.

The level of titanium in the ore and sediment at Osiri B is 10,767 ± 825 mg/kg and 13,000 ± 956 mg/kg respectively (as shown in Table 11); these are the highest in all the mines.

Table 5. Elemental concentration of ore and sediment from Osiri B (mg/kg).

Element	Osi-O1	Osi-O2	Osi-O3	Osi-O4	Osi-S1	Osi-S2	Osi-S3	Osi-S4
K	9787 ± 1740	1333 ± 231	14867 ± 1960	7583 ± 755	2385 ± 391	8753 ± 1653	15350 ± 2025	11653 ± 1813
Ca	22000 ± 1743	3200 ± 250	27633 ± 2073	715 ± 247	6967 ± 517	17733 ± 1460	42100 ± 2985	16767 ± 142
Ti	10767 ± 825	1589 ± 125	9090 ± 716	2475 ± 209	2803 ± 218	10633 ± 801	9280 ± 736	13000 ± 956
Cr	659± 102	158 ± 22	607 ± 99	283 ± 41	268 ± 37	769 ± 104	645± 105	811± 111
Mn	934 ± 80	670 ± 47	2973 ±207	2255 ± 152	1028 ± 73	2880 ± 200	3140 ± 218	3820 ± 261
Fe	93867 ± 6083	30518 ± 1981	90333 ± 5863	51250 ± 3332	54333 ± 3515	110000 ± 7127	98900 ± 6410	116000 ± 7530
Co	736 ± 87	509 ± 57	766 ± 85	752 ± 85	1010 ±106	889 ± 93	865 ± 91	872 ± 97
Cu	<40	<40	48.37 ± 10.64	44.65 ±10.95	49 ± 12	44 ± 10	47 ± 11	51 ± 2
Zn	104 ± 11	62 ± 7	110 ± 17	58 ± 9	86 ± 11	89 ± 11	83 ± 10	101 ± 12
As	191 ± 14	806 ± 53	105 ± 9	118± 10	270 ± 19	229 ± 16	172 ± 13	191 ± 14
Au	20 ± 6	14.07 ±4.46	<10	17± 6	<10	<10	<10	25 ± 6
Hg	<2	<2	<2	<2	<2	<2	<2	<2
Pb	20 ± 4	16 ± 3	22 ± 4	30 ± 5	28 ± 5	23 ± 4	52 ± 5	29 ± 4
Rb	33 ± 3	24 ± 2	37 ± 3	91 ± 7	39 ± 4	22 ± 2	39 ± 3	35 ± 3
Sr	49 ± 4	84 ± 6	87 ± 6	53 ± 4	141± 10	58 ± 4	93 ± 6	70± 5
Y	19 ± 2	21 ± 2	18 ± 2	28 ± 3	29 ± 3	16 ± 1	16 ± 2	21 ± 2
Zr	211 ± 14	125 ± 9	135 ± 9	239 ± 16	158 ± 11	96 ± 6	130 ± 9	193 ± 13
Nb	34 ± 3	14 ± 1	20 ± 2	21 ± 2	12 ± 2	10 ± 1	16 ± 1	28 ± 2

Key: O-ore; S- Sediment.

Gold, the main mineral of interest in the Migori gold mining belt, is found in almost all the ore and sediment samples collected from the four mines. The concentration of gold is particularly enhanced in the ore and sediment samples collected from Mikei with the highest gold concentration registered being 73 ± 7 mg/kg in one sediment sample (see Table 6). The presence of gold in the sediments confirms the poor extraction methods used by the artisanal miners in the extraction of gold.

Table 6. Elemental concentration in ores and sediments from Mikei (mg/kg).

Element	Mik-O1	Mik-S1	Mik-S2	Mik-S3	Mik-S4
K	<350	3702 ± 765	7757 ± 1665	3293 ± 519	23509 ± 1777
Ca	6668 ± 734	3955 ± 453	3786 ± 765	1680 ± 249	5797 ± 651
Ti	1191 ± 216	711 ± 142	4242 ± 427	1062 ± 122	2594 ± 249
Cr	259 ± 61	257 ± 46	691 ± 101	279 ± 38	415 ± 67
Mn	176 ± 29	362 ± 34	1019 ± 85	476± 38	399 ± 36
Fe	9092 ± 596	16772 ± 1091	65113 ± 4226	32267 ± 2095	21660 ± 928
Co	<58	164 ± 33	534 ± 77	408 ± 56	155 ± 30
Cu	845 ± 58	184 ± 16	208 ± 21	303 ± 24	<40
Zn	<35	215 ± 17	755 ± 53	1227 ± 82	150 ± 10
As	222 ± 16	316 ± 24	2980 ± 195	4095 ± 268	5705 ± 242
Au	21 ± 5	27 ± 23	41 ± 10	33 ± 9	73 ± 7
Hg	<2	16 ± 6	35 ± 8	32± 8	62 ± 7
Pb	28.28 ± 4.37	403 ± 28	1833 ± 120	3548 ± 231	109 ± 7
Rb	24 ± 3	26 ± 3	29 ± 3	33 ± 4	89 ± 4
Sr	126 ± 9	130 ± 9	93 ± 7	108 ± 8	16 ± 86
Y	<6	7 ± 2	21 ± 3	31 ± 4	12 ± 1
Zr	55 ± 4	65 ± 5	193 ± 13	110 ± 8	146 ± 8
Nb	<3	<3	18 ± 2	<3	5.26 ± 1

Key: O- Ore; S- Sediment

Mercury which is used in the amalgamation in the gold extraction process is found in larger quantities in sediments compared to ores. It is interesting to note that the level of mercury in the sediments from Osiri A and Macalder were

45

found to be below detection limit (see Tables 4, 5 and 8). This could be due to the duration the sediments at these mines had been kept after they were removed from the panning ponds awaiting reprocessing. The high density of mercury allows gold and gold mercury amalgam to sink to the bottom of the panning pond or river while sediment is washed away (Alpers *et al.*, 2005).

Table 7. Elemental concentration in ore and sediment from Masara (mg/kg).

	Mas-O	Mas- S
Element		
K	6285 ± 1437	5950 ± 1420
Ca	5825 ± 761	5700 ± 754
Ti	1822 ± 272	<165
Cr	349 ± 74	294 ± 71
Mn	317 ± 39	168 ± 30
Fe	27106 ± 1645	11600 ± 760
Co	209 ± 41	101 ± 27
Cu	229 ± 18	30 ± 7
As	400 ± 26	231 ± 16
Au	24 ± 6	20 ± 3
Hg	<2	16 ± 4
Pb	<23.07 ± 4.24	20 ± 3
Rb	25 ± 3	<11
Sr	189 ± 12	56 ± 4
Zr	69 ± 4	14 ± 1

Key:

O- Ore; S- Sediment

Table 8. Elemental concentration of ore and sediment from Osiri A (mg/kg).

Element	Osi-O1	Osi-O2	Osi-S1	Osi-S2
K	<350	9323 ± 3593	4965 ± 755	2447 ± 417
Ca	96569 ± 6430	25000 ± 9426	1918 ± 338	824 ± 186
Ti	2445 ± 361	7607 ± 2834	1905 ± 192	1214 ± 120
Cr	695 ± 105	482 ± 212	323 ± 47	178 ± 30
Mn	1109 ± 91	1517 ± 575	1263 ± 90	987 ± 70
Fe	21782 ± 1419	88033 ± 3290	38700 ± 2512	28833 ± 1874
Co	224 ± 44	902 ± 361	515 ± 66	389 ± 51
Cu	<40	127 ± 49	128 ± 14	174 ± 16
Zn	98 ± 11	298 ± 118	99 ± 11	98 ± 10
As	881 ± 58	29.30 ± 13.91	853 ± 57	373 ± 26
Au	<10	<10	25 ± 7	20 ± 6
Hg	<2	<2	<2	<2
Pb	29.95 ± 4.81	131 ± 52	305 ± 21	121 ± 10
Rb	<11	48 ± 19	44 ± 4	44 ± 4
Sr	111 ± 8	70 ± 27	90 ± 6	87 ± 7
Y	5.28 ± 1.26	21 ± 8	15 ± 2	15 ± 2
Nb	<3	25 ± 10	22 ± 2	22 ± 2

Key:

O- Ore; S- Sediment

Toxic elements like lead, zinc and arsenic were also found in almost all the mines. At Mikei (Table 6) for instance the average levels of arsenic, lead and

zinc were found to be 3274 mg/kg, 1473 mg/kg and 587 mg/kg respectively. These levels are higher than levels found in the sediments in Adola regions of Southern Ethiopia which were 60 mg/kg, 65 mg/kg and 106 mg/kg for arsenic, lead and zinc respectively (Gataneh and Alemayehu, 2006). The presence of arsenic in the area shows the existence of arsenopyrite ($FeAsS_2$) which has always presented a problem in the extraction of gold. Arsenic and gold are often related in hard rock gold mines where often gold occurs as tiny blobs within the arsenopyrite.

Arsenic is a danger to the miner's health and even animals: it is a carcinogen that causes both skin and lung cancer. Other effects of arsenic include cardiovascular and celebrovascular disease, Reynaud's phenomena, hepatophathy and nephropathy, malignant neoplasm including Bowen's disease (Ogola *et al.*, 2002). However this high level should also be exploited if the concentration is economically viable since pure arsenic metal is used to produce crystalline gallium arsenide which is a semiconductor used in computing and electronic industries. Arsenic is also used in agriculture, livestock and general industries (Weast, 1968). Lead which is also one of the toxic metals even at low levels and a carcinogen was present in high levels at Mikei, Macalder and Masara but absent in samples from Osiri. The presence of these toxic elements could have been contributing to the unknown illnesses and deaths that have been reported among the gold miners over the years.

There seems to be a positive correlation between the concentration of cobalt and iron from all the four mines, they both appear in all the mines and as the concentration of one increases so does the other. This could possibly be due to the fact that they originate from the same rock formation.

Yttrium, niobium and rubidium were also found in most of the mines however they were at concentrations below 100 mg/kg. Thorium was only detected in samples Mikei mine.

4.2.2 Water samples

Copper, zinc and iron were found in all the water samples collected from the four mines. The highest concentration of copper, zinc and iron were 14,976 ± 616 µg/l, 683 ± 33 µg/l and 77, 903 ± 203 µg/l respectively (see Table 9). A typical ED-XRF spectrum analysis of a water sample is shown (Figure 12).
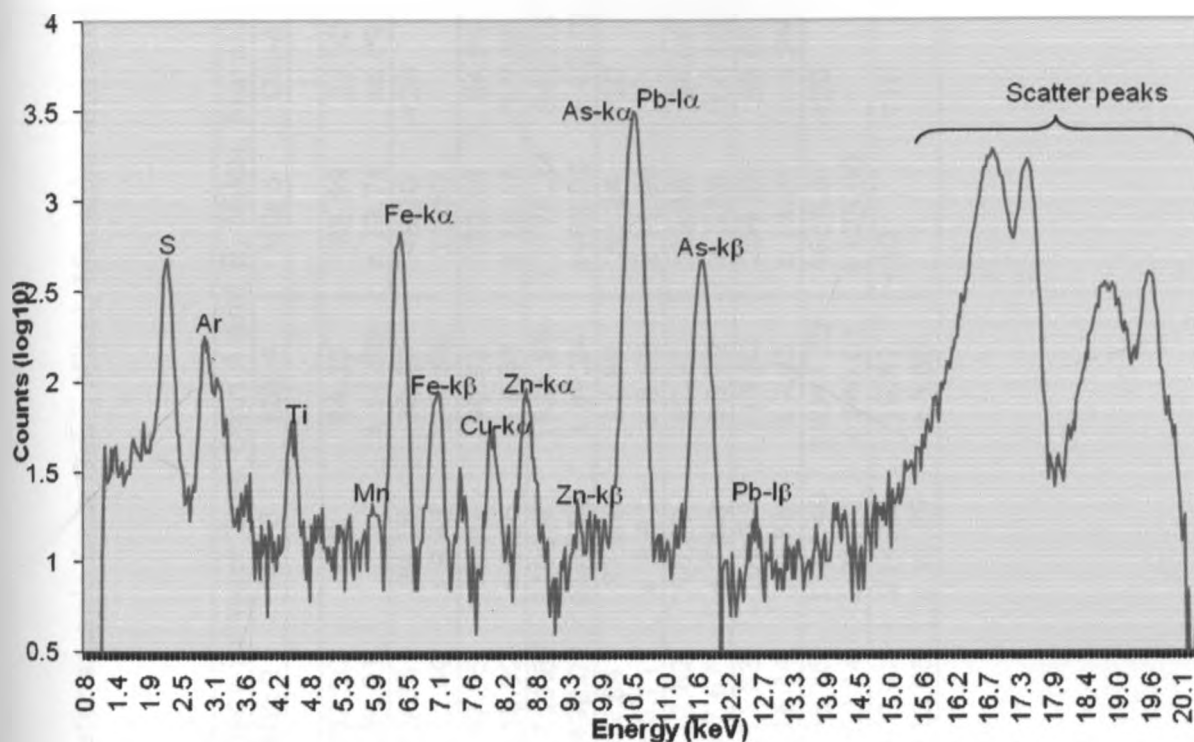
Figure 12. Typical ED-XRF spectrum of a water sample.

Toxic element zinc was detected in all the water samples while other toxic elements like arsenic and lead were only found in water samples from Mikei, Masara and Macalder. Arsenic was the highest among the toxic elements, detected in Mikei; 18,048 ± 746 µg/l while the highest levels of lead and zinc were 215 ± 16 µg/l and 683 ± 33 µg/l respectively. The concentrations of arsenic in the water samples analyzed in the present study are much higher (about two hundred times more) than those reported from Adola region in

Table 9. Elemental concentration in water sample from Osiri, Mikei, Macalder and Masara (µg/l).

Element	Elemental concentrations in water from Osiri A and B, Mikei, Macalder and Masara										
	Mas 1	Mac 2	Mik 1	Mik 2	Mik 3	Mik 4	Mik 5	Osi-A	Osi-B 1	Osi- B2	Osi-B3
Ti	<30	112.88 ± 5.13	46.48 ± 11.26	207.50 ± 24.91	<30	84.33 ± 11.65	185.59 ± 13.76	23.90 ±6.89	<30	<30	<30
Cr	144.85 ± 25.17	<25	22.37 ± 7.46	69.35 ± 12.49	39.15 ± 8.45	30.20 ± 9.86	48.10 11.30	<25	<25	<25	<25
Mn	339.77 ± 5.72	35.04 ± 8.45	<15	157.95 ± 15.92	78.21 ± 8.26	46.72 ± 8.97	132.55 ± 15.10	34.54 ± 7.25	<15	<15	28.95 ± 8.22
Fe	77903.08 ± 203.10	1174.78 ± 66.87	1153.69 ± 97.43	11710.87 ± 492.07	3100.97 ±148.03	1834.55 ± 89.24	11775.34 ±493.95	849.55 ± 42.70	520.68 ± 40.57	261.56 ±29.70	360.50 ± 32.68
Co	1014.11 ± 72.68	<10	<10	62.84 ± 6.71	37.51 ± 8.61	27.89 ± 8.63	51.94 ± 11.96	<10	<10	<10	<10
Cu	14975.59 ± 616.14	45.31 ± 6.71	92.96 ± 9.50	113.62 ± 7.67	70.89 ± 7.56	67.37 ± 5.92	62.68 ± 5.56	34.04 ± 4.63	29.34 ± 5.01	30.05 ± 4.23	34.74 6.99
Zn	444.22 ± 21.76	683.15 ± 32.93	169.83 ± 21.66	291.33 ± 16.14	102.53 ± 6.85	113.82 ± 7.65	238.26 ± 13.94	33.65 ± 4.29	56.46 ± 4.29	34.10 ± 6.94	44.04 ± 8.41
As	<20	58.16 ± 15.59	<20	958.16 ± 60.14	1184.40 ± 78.77	18047.52 ± 746.01	4058.87 ± 175.00	<20	<20	<20	<20
Pb	88.11 ± 9.64	24.09 ± 4.76	<10	200.91 ± 13.05	214.53 ± 16.29	19.51 ± 5.50	<10	<10	<10	<10	<10

Ethiopia where the average concentration of arsenic was found to be 93 µg/l (Getaneh and Alemayehu, 2006). However higher values have been reported elsewhere e.g. 72 mg/l registered at the Iron Duke mine in Zimbabwe (Williams and Smith, 2000). Lead which is also one of the toxic metals even at low levels and a carcinogen was present in high levels at Mikei, Macalder and Masara. It was noted that the miners don't drink these waters but they are used for cleaning e.g. washing their hands. Livestock including cows, goats and sheep in many occasions especially during dry periods also drink water from these pools. The situation is worsened when the contaminated water find its way to nearby rivers that have direct domestic use by the locals.

4.2.3 Dust samples

Table 10. Elemental concentration in dust from Masara and Mikei (µg/m^3).

Element	Mas-01	Mik-01	Mik-02	Mik-03	Mik- average.
Cr	<3	<3	4 ± 1	<3	<3
Mn	8 ±1	4 ± 1	6 ± 1	4 ± 1	5 ± 1
Fe	98 ± 6	40 ± 3	51 ± 3	22 ± 2	38 ± 3
Cu	<2	<2	<2	<2	<2

Manganese and iron were found in all the dust samples collected from the two sites as shown in Table 10 above. The highest iron concentration was found at Masara, 98 ± 6 µg/m^3 while at Mikei iron concentration ranged from 22 ± 2 to 51 ± 3 µg/m^3 with a mean of 37 ± 9 µg/m^3. Concentration of manganese on the other hand ranged from 4 ± 1 to 6 ± 1 µg/m^3 with a mean of 5 ± 1 µg/m^3 at Mikei. Copper and chromium were also present in some of the dust samples. It is noticeable that most of the toxic metals like arsenic, lead and zinc were not detected in the dust samples even though they were present in both the ore and sediment samples from these mines.

51

4.3 Activity concentration of radionuclides

4.3.1 ^{226}Ra in water samples

The results of liquid scintillation analysis shows that ^{226}Ra and its decay products namely ^{222}Rn, ^{214}Pb, etc are not above the detection limit of 0.94 kBqm^{-3} in any of the mine water samples.

4.3.2: ^{40}K, ^{226}Ra and ^{232}Th in ore and sediments

The activity concentrations of ^{40}K ranges from 80 Bq/kg to 413 Bq/kg, with a mean value of 100 Bq/kg, ^{226}Ra ranges from 12 Bq/Kg to 145 Bq/kg with a mean value of 25 Bq/kg and ^{232}Th ranges from 21 Bq/kg to 258 Bq/kg with the mean of 40 Bq/kg as shown in the Table 10: ^{40}K had the highest activity concentration. All these average values are lower than the world wide average concentrations of ^{40}K, ^{226}Ra and ^{232}Th which are 400, 35 and 30 Bq/kg respectively as reported by UNSCEAR (2000).

Table 11. Activity concentration of radionuclides in sediment and ore samples from Osiri, Mikei, Macalder and Masara (Bq/Kg).

Sample	Activity concentration (Bq/Kg)		
	^{40}K	^{226}Ra	^{232}Th
Osi B O_1	239.76 ± 30.22	<10.42	<13.47
Osi B O_2	167 ± 26.10	<10.42	<13.47
Osi B O_3	<42.50	<10.42	258.04 ± 36.32
Osi B O_4	100.33± 21.38	145.06 ± 8.40	129.25 ±27.70
Osi A O_1	<42.50	<10.42	60.34 ± 20.93
Osi A O_2	413.34 ±27.31	58.13 ± 6.17	<13.47
Mac O_1	<42.50	<10.42	47.12 ± 23.50
Mac O_2	<42.50	14.00 ± 4.67	<13.47
Mac O_3	80.20±16.00	<10.42	<13.47
Mac O_4	<42.50	<10.42	<13.47
Mac O_5	<42.50	<10.42	21.41± 5.23
Mik O_1	<42.50	35.60 ± 6.00	105.31 ± 25.25
Mas O_1	161.38 ± 25.25	<10.42	73.99 ± 27.69
Osi BS_1	<42.50	13.53 ± 6.46	<42.50
Osi BS_2	217.94 ± 24.86	12.26 ± 6.32	21.76 ± 8.24
Osi B S_3	156.39 ± 4.55	38.76	<13.47
Osi B S_4	<42.50	<10.42	39.38 ± 39.08
Osi A S_1	1798.93 ± 22.35	23.00 ± 7.21	<13.47
Osi A S_2	166.70 ± 23.00	48.21 ± 6.73	<13.47
Mac S_1	<42.50	<13.47	<13.47
Mac S_2	<42.50	41.99 ± 5.29	<13.47
MiK S_1	<42.50	29.10 ± 6.27	86.43 ± 24.98
Mik S_2	<42.50	<10.42	22.27 ± 21.41
Mik S_3	83.89 ± 22.14	18.19 ± 6.35	23.42 ± 22.51
Mik S_4	<42.50	39.30 ± 7.17	<13.47
Mas S_1	83.10 ± 81.96	<10.42	<13.47

The activity concentration of ^{226}Ra, ^{232}Th and ^{40}K were compared to determine any trend or correlation. The results show positive but weak correlations between the radionuclides as illustrated by Figures 13-15.

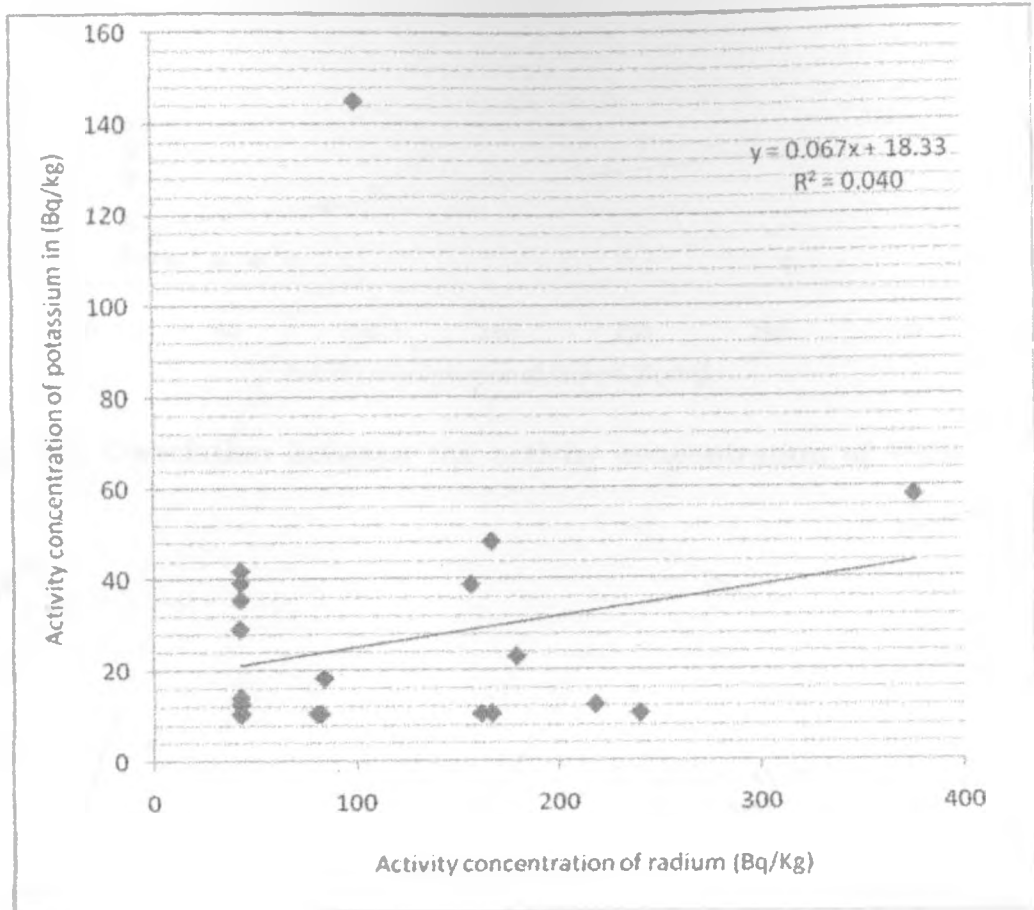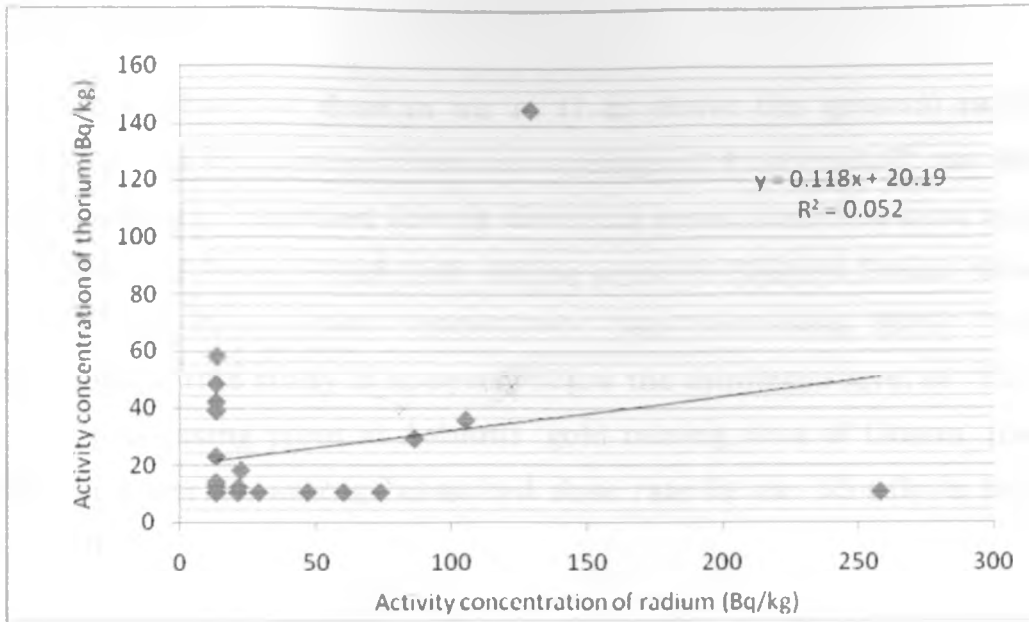**Figure 13.** Correlation between the activity concentration of ^{40}K and ^{226}Ra.

Figure 14. Correlation between the activity concentration of [232]Th and [226]Ra.
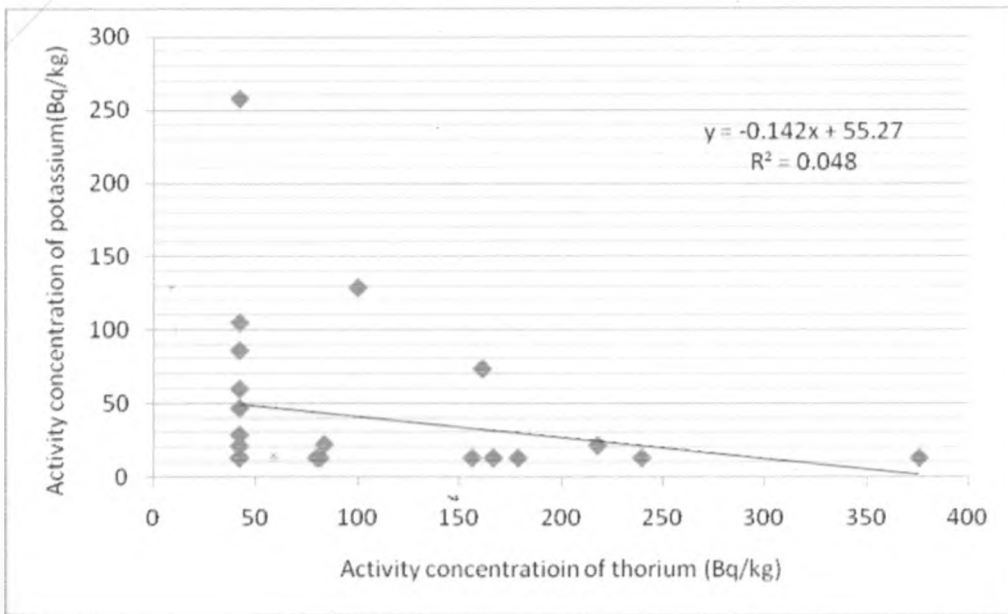
Figure 15. Correlation between the activity concentration [40]K and [232]Th.

4.4 Absorbed dose

The calculated absorbed dose in air at (1 m above the ground) range from 16.14 nGy/h to 178.11 nGy/h with an average of 42.11 nGy/h as shown in Table 11. This mean absorbed dose is above the mean absorbed dose registered at Aassedakh and Hadal Autab gold mining areas in Eastern Sudan which was 19 ± 7 nGy[-1] and 7 ± 6 nGyh[-1] respectively (Sam and Awad, 2000). The mean absorbed dose in this study is however, below the minimum level of 55 nGy/h found in a processing plant at Ashanti gold mining area of Ghana, (Darko *et al.*, 2005) and world's average absorbed dose rate in air, 55 nGy/h (Sam and Awad, 2000).

Table 12. Calculated absorbed dose from Osiri, Mikei, Masara and Macalder (nGy/h).

Sample	Absorbed dose (nGy/h)
Osi B O_1	23.51 ± 20.126
Osi B O_2	20.44 ± 1.10
Osi B O_3	178.11 ±15.58
Osi B O_4	152.52 ± 26.05
Osi A O_1	46.44 ± 8.97
Osi A O_2	51.27 ± 18.45
Mac O_1	37.63 ± 10.08
Mac O_2	16.76 ± 0.20
Mac O_3	16.09 ± 10.66
Mac O_4	<15.23
Mac O_5	20.51 ± 2.24
Mik O_1	87.16 ±18.55
Mas O_1	60.53 ± 28.72
Osi BS_1	16.14 ± 0.27
Osi BS_2	28.91 ± 20.36
Osi B S_3	32.17 ± 16.65
Osi B S_4	25.62 ± 16.77
Osi A S_1	26.78 ± 15.18
Osi A S_2	33.93 ±15.40
Mac S_1	<15.23
Mac S_2	39.74 ± 0.22
MiK S_1	71.83 ± 14.89
Mik S_2	20.52± 9.18
Mik S_3	26.32 ±25.17
Mik S_4	27.62 ± 0.31
Mas S_1	81.96 ± 54.58

4.5 Dust loading

The total dust loading at Masara and Mikei was found to be 3.67 and 1.33 mg/m^3 respectively. The dust loading at Masara is less than values reported at drilling and blasting sites in Tanzanite gemstone mines, 28.4 mg/m^3 (Braveit et al., 2002). The high dust level at Masara could have been due to the high number of miners who were crushing the ore at Masara at the time of dust collection but it could also be due to the positioning of the air sampler as well as the direction of wind at the crushing site among other factors at the dust collection time. It was noted that since the fixed method was the only technique used to collect dust, the dust collected reflects only the average dust concentration in the area and not the exposure of any particular worker at the site (Biffi and Belle, 2003). It also is noted that while the fixed air sampling method has sometimes been used to estimate workers exposure by dust inhalation, it is now considered that, if the dose estimate will be based on air sampling, the air samples should be representative of the air breathed by the worker. To estimate internal doses, personal air samplers are preferred to fixed air samplers (Van der Steen and Van Weers, 2004).

4.6 Calculation of the annual effective dose due to different exposure pathways

The calculated effective dose due to different pathways is presented as shown below where:

D_{ext} is the external dose due to γ- rays emitted by radionuclides contained in the environment.

D_{inh} is the internal dose due to the inhalation of air contaminated with dust from the ore.

D_{ing} is the internal dose due to inadvertent ingestion of radionuclides.

E_T The total exposure from various pathways

58

Table 13. Calculated effective dose to the artisanal miners due to different exposure scenarios and pathways (Sv/yr, unless stated otherwise).

Scenario	Effective dose according to pathway			
	External irradiation (D_{ext})	Inhalation (D_{inh})	Ingestion (D_{ing})	Total effective dose E_T ($\mu Sv/yr$)
Digging	5.49×10^{-7}	-	1.83×10^{-7}	0.73
Panning	5.49×10^{-7}	-	1.83×10^{-7}	0.73
Crushing	1.82×10^{-7}	3.76×10^{-6}	2.52×10^{-7}	4.19

The total effective dose received from digging and panning was 0.73 µSv/yr while total effective dose received from crushing was 4.19 µSv/yr as shown in Table 13. The values are lower than the annual effective dose registered in gold mines in Ghana and Sudan which were 0.23- 0.28 mSv/yr (Darko *et al.*, 2005) and 0.04 – 0.2 mSv (Sam and Awad, 2000) respectively. All values are below 20 mSv/yr, which is the annual effective dose limit for occupationally exposed (radiation) worker (IAEA, 1996) and 5 mSv/yr, the maximum annual dose to surface workers in gold mines in South Africa (Van der Steen and Van Weers, 2004). However, care must be taken since it is believed that radiation at any level poses a risk. It is also observed that the most important exposure scenario is ore-crushing.

The most significant pathway is inhalation of the auriferous ore dust while the least significant is the external exposure from submersion in the auriferous contaminated dust. A study conducted by Mustapha *et al.* (2007) on the occupational radiation exposures of the artisans mining columbite-tantalite in the Democratic Republic of Congo also show similar concentration trend. Similar results were also found in a phosphate industry in Egypt (Abbady *et al.*,

59

2005). Contributions to the total effective dose from hand and skin exposures due to the handling of ore, ore dust and the slurry were not considered in this study.

CHAPTER FIVE

5.0 Conclusion and recommendations

The activity concentrations of the radionuclides as well as the annual absorbed dose was found to be below the worlds average while presence of toxic elements like arsenic, lead and zinc were noted. Inhalation of the gold ore dust was found to be the worst exposure pathway with crushing being the worst exposure scenario.

5.1 Conclusions

The level of radioactivity in the ore and sediments were found to be below the global average level.

Mine waters examined contain low levels of ^{226}Ra and should not pose any significant radiological problem.

The dust loading at the crushing sites is relatively high.

The absorbed dose in air due to gamma – rays emitters in the mines was found to be lower than the worlds average outdoor exposure value of 55 nGy/h.

The annual effective dose in the mines is below 1 mSv/yr and 20 mSv/y, the limits for the general public and radiation worker respectively.

Among the working scenarios, crushing has the highest potential of exposure scenario and the highest exposure pathway is the inhalation of contaminated dust.

61

High levels of well known toxic elements such as arsenic, lead and zinc were also recorded in this study.

5.2 *Recommendations*

Based on the results and conclusions drawn from this study the following are recommended:-

Precautionary steps such as wearing protective clothing and masks should be taken since the level of dust in then crushing sites is high. The miners should also be encouraged to put on clothes during mining especially during crushing.

The levels of toxic elements like lead, arsenic and zinc in the mines are very high therefore the miners may need to take precaution e.g. maintain personal hygiene practices such as washing of hands thoroughly at meal times etc. The miners should also avoid mixing home utensils with the equipments used in the mines in order to decrease possible exposure pathway. Access of the members of the public to the mines and mine tailings should be minimized to prevent the members of the public from dispersing them or using them for building etc.

Further research should be carried out to confirm the exact levels of copper, titanium and arsenic with a view of exploiting them if they are economically viable.

More samples of dust, ore, sediments and water should be collected for analysis to get a more representative result. The samples should also be collected at different times of the year.

Measurement of respirable dust particles should be carried out, rather than the total dust loading as this will provide a more representative value of the internal exposure. Measurement of the dust loading should be carried out with

large volume samplers and the measurement carried out over longer period of time as this will give more meaningful results.

Though contamination of the rivers by the toxic elements in the area had been carried out by Ogola *et al.* (2002), a study of the concentration of these elements should be done further downstream to ascertain their levels as these rivers flow away from the mining areas. A study should also be carried out to determine the level of mercury in the blood of the miners and the people living around these mines.

The government should recognize the artisanal miners and provide them with well structured laws of operation. Clear policies on mining that pay closer attention to the effects of mining to the environment should be put in place. Rehabilitation of the mines needs to be emphasized and the government should hold the miners responsible for any environmental pollution during and after mining.

CHAPTER SIX

6.0 REFERENCE.

Abbady, A.G.E., Uosif, M.A.M. and El-Taher, A. (2005) Natural Radioactivity and dose assessment for phosphate rocks from Wadi El-Mashash and El-Mahamid Mines, Egypt, *Journal of Environmental Radioactivity* **84**: 65-78.

Alpers N., Hunerlach M.P., May J. T. and Hothem R.L. (2005) Mercury contamination from Historical Gold Mining in California, USGS Fact sheet 2005-3014 Version 1.1.

Amutabi, M. and Lutta-Mukhebi M. (2001) Gender and mining in Kenya: The case of Mukibira mines in Vihiga District. Jenda: A journal of Culture and African Women Studies. 1530-5686.

Banzi, F.P., Kifanga, L.D. and Bundala, F.M. (2000): Natural Radioactivity and Radiation exposure at the Majingu phosphate mine in Tanzania, J. Radiol. Prot. **20:** 41-51.

Bermùdez, O. (1999) The mineral industry of Kenya. U.S. Geological Survey year book.

Biffi, M. and Belle, B.K. (2003) Quantification of dust generating sources in Gold and Platinum mines, Report by the safety in Mines Research Advisory Committee.

Bowel, R.J, Warren, H.A., Minjera, H.A. and Kimaro, N. (1995) Environmental impact of former gold mining on the Orangi river, Serengeti N.P., Tanzania, Biogeochemistry **28:** 131-160.

Bratveit, M., Moen, B.E., Mashalla Y.J.S. and Maalim, H. (2002) Dust Exposure During Small-Scale Mining in Tanzania: A pilot Study, *Ann. Occup. Hyg, 47(3): 235-240.*

Carvalho, F.P., Madruga, M.J., Reis, M.C., Alves, J.G., Oliveira, J.M. Gouveia, J. and Silva, L. (2007) Radioactivity in the environment around past radium and uranium sites of Portugal, *Journal of Environmental Radioactivity* **96**: 39-46.

Darko, E.O., Tetteh, G.K. and Akaho E.H.K. (2005) Occupational Radiation Exposure to NORMS in Gold Mine, *Radiation Protection Dosimetry* **114**(4):538- 545.

Deb M., Tiwari G. and Lahiri-Dutt K. (2008) Artisanal and small scale mining in India: Selected studies and overview of the issues. *International journal of mining, reclamation and environment:* 1-16.

Eckerman, K. F. and Ryman J.C. (1993) Federal Guidance Report Number: No. 12: External exposure to radionuclides in air, water and soil (Washington, DC: US Environmental Protection Agency Office of Radiation and Indoor Air) EPA 402-R-93-081.

Getaneh, W. and Alemayehu T. (2006) Metal contamination of the environment by placer and primary gold mining in the Adola region of Southern Ethiopia, *Environmental Journal* **50**: 339-352.

Haridasan, P.P., Pillai, P.M.B., Khan A.H. and Puranik V.D. (2006) Natural Radionuclides in Zircon and Related Radiological impacts in the mineral separation Plants, *Radiation Protection Dosimetry* **121**(4): 364-369.

Hentschel, T., Hrushka, F and Prieste, P. (2002) Global report on Artisanal and Small – Scale mining. Report commissioned by Mining, Minerals and Sustainable Development (MMSD) project of International Institute for Environment and Development (IISD), England, Report No. 70.

Hilson G. (2002) The environmental impact of small scale gold mining in Ghana: Identifying problems and possible solutions, *Geographical Journal* **168**: 57-72.

Hutchson, R.W (1981) Report on UNRFNRE Exploration project, Migori Goldbelt, Kenya pp22.

ILO (1999) Social and Labour Issues in small scale mining. ILO, Geneva.

IAEA (1996) International Basic Safety Standards for Protection against Ionizing Radiation and for the Safety of radiation Sources, Safety Series No. 115 (Vienna: IAEA).

ICRP (1994) Dose coefficients for intakes of Radionuclides by workers ICRP, Ann. ICRP **24** (4) (Oxford: Pegamon).

Keays, R.R. (1982) Archean gold deposits and their source rocks. The Upper Mantle Connection, in: *Proceedings of the Symposium* 'Gold 82', Zimbabwe, pp.17-51.

Knoll, G.F. (1979) Radiation detection and measurements, John Willey and sons, New York.

Lipsztein, J.L.,Dias da Cunha, K. M., Azeredo, A.M. G., Julião, L., Santos, M., Melo, D. R. and Simeões Filho, F.F.L. (2001) Exposure of workers in mineral processing industries in Brazil, Journal of Environmental Radioactivity **54:** 189-199.

Mustapha A.O., Mbuzukongira P. and Mangala M.J. (2007) Occupational radiation exposures of artisans mining columbite-Tantalite in Eastern Democratic Republic of Congo, *J. Radiol. Prot.* **27**: 187- 195.

Mustapha, A.O. (1999) Assessment of Human Exposures to Natural Sources of Radiation in Kenya, PhD thesis, University of Nairobi, Kenya.

Oatway, W. B. and Mobbs S.F. (2003) Methodology for estimating the dose to the members of the public from the future use of land previously contaminated with radioactivity NRPB-W36 Report (Chilton: NRPB).

Ogola J.S. (1987) Mineralization in the Migori Greenstone belt, Macalder Western Kenya, Journal of Geology 22. pp 25-44.

Ogola J.S., Mutulah W.V.and Omullo M.A. (2002) Impact of gold mining in the environment and human heath: A case study in Migori Goldbelt, Kenya. *Environmental Geochemistry and health* **24**: 141-158.

Omar, M., Suleiman I., Hassan, A. and wood, A. H., (2007) Radiation dose assessment at Amang processing plants in Malaysia, *Radiation Protection Dosimetry.* **124**(4): 400-4007.

Oyedele, J.A. (2006) Assessment of the Natural radioactivity in the Soils of Windhoek City, Namibia, Southern Africa, *Radiation Protection Dosimetry* **121**(3):337-340.

Rösner, T. and Schalkwtk, A. (2000) The environmental impact of gold mine tailings footprints in the Johannesburg region, South Africa, Bull Eng Geol Env **59**: 137-148.

Phillips 1981: The periodic Table of elements, Netherlands, Almelo.

Sam, A.K. and Awad A.A.M.M. (2000) Radiological Evaluation of Gold Mining activities in Ariab (Eastern Sudan), *Radiation Protection Dosimetry* **88** (4): 335-340.

Sam, A.K. and Elmahadi M.M. (2008) Assessment of absorbed dose rate in air over Plowed Arable lands in Sinnar State, Central Sudan, *Radiation Protection Dosimetry* **129** (4): 473-477.

Sanders, L.D. (1964) Copper of Kenya, Geology survey of Kenya, Memoir No. 4 Nairobi: Page 51.

Schackleton, R.M. (1946) Geology of Migori Gold Belt and adjoining areas. Geology survey of Kenya, Report No. 10, Nairobi, Page 60.

Sparks C.J. (1979) Rapid quantitative X-ray fluorescence using fundamental parameters method. Advances in X-ray analysis. Plenum Press. New York pp 109.

Tahir, S.N.A., Jamil, K., Arif, M., Ahmed, N. and Ahmad, S.A (2005) Measurement of Activity Concentrations of Naturally occurring Radionuclides in Soil Samples from Punjab Province of Pakistan and Assessment of Radiological Hazards, *Radiation Protection Dosimetry.* **113** (4): 421-427.

UNSCEAR (1993): Sources and Effects of Ionizing Radiation. Report to the General assembly with annexes. NY.

UNSCEAR (2000) Report to the General assembly. Annex B: exposures from natural radiation sources. (New York.)

Van der Steen, J. and Van Weers, A.W. (2004) Radiation protection in NORM industries *11th Int. Congress of the International Radiation Protection Association IRPA 11 (Madrid, Spain, May* 2004).

Veiga M. M. and Hinton J. (2002) Abandoned artisanal gold mines in Brazilian Amazon: A legacy of mercury contamination, Natural resources forum **26**: 15-26.

Weast C. Robert (1968) Handbook of Chemistry and Physics 49th edition. The chemical Rubber Company, USA.

Wendel, G. (1998) Radioactivity in mines and the mine water- sources and mechanisms. *The Journal of The South African Institute of Mining and Metallurgy.* 87-92.

Williams, T.M. and Smith B. (2000) Hydrochemical characterization of acute mine drainage at Iron Duke, mine, Mazowe, Zimbabwe, *Environmental Geology* **39**: 272-279.

Winde F. and Sandham L.A. (2004) Uranium pollution of South African streams – An overview of the situation in gold mining areas of Witwatersrand, *Geo. journal* **61**: 131-149.